



HAL
open science

Oxygen, Carbon and pH Variability in the Indian Ocean

Raleigh R Hood, Tim Rixen, Marina Lévy, Dennis A Hansell, Victoria J Coles, Zouhair Lachkar

► **To cite this version:**

Raleigh R Hood, Tim Rixen, Marina Lévy, Dennis A Hansell, Victoria J Coles, et al.. Oxygen, Carbon and pH Variability in the Indian Ocean. Oceanography of the Indian Ocean, Elsevier, In press. hal-03917888

HAL Id: hal-03917888

<https://cnrs.hal.science/hal-03917888v1>

Submitted on 6 Feb 2023

HAL is a multi-disciplinary open access archive for the deposit and dissemination of scientific research documents, whether they are published or not. The documents may come from teaching and research institutions in France or abroad, or from public or private research centers.

L'archive ouverte pluridisciplinaire **HAL**, est destinée au dépôt et à la diffusion de documents scientifiques de niveau recherche, publiés ou non, émanant des établissements d'enseignement et de recherche français ou étrangers, des laboratoires publics ou privés.

Oxygen, Carbon and pH Variability in the Indian Ocean

Raleigh R. Hood, Horn Point Laboratory, University of Maryland Center for Environmental Science, Cambridge, MD, 21613, USA

Tim Rixen, Leibniz Centre for Tropical Marine Research, University of Bremen, Bremen, 28359, Germany

Marina Levy, LOCEAN-IPSL, Sorbonne University, 75252 Paris Cedex 05, France

Dennis A. Hansell, Rosenstiel School of Marine and Atmospheric Science, University of Miami, 4600 Rickenbacker Causeway, Miami, FL 33149, USA

Victoria J. Coles, Horn Point Laboratory, University of Maryland Center for Environmental Science, Cambridge, MD, 21613, USA

Zouhair Lachkar, Center for Prototype Climate Modeling, New York University, Abu Dhabi, PO Box 129188, Saadiyat Island, Abu Dhabi, United Arab Emirates

Abstract

This chapter provides an overview of the physical and biogeochemical factors that control spatial and temporal patterns of oxygen minimum zones (OMZs), carbon and pH variability in the Indian Ocean. Oxygen concentrations decline to nearly zero in Arabian Sea intermediate water with profound biogeochemical impacts on the nitrogen cycle as a result of denitrification. These impacts can hardly be observed in the Bay of Bengal where oxygen concentrations are poised just above the threshold below which denitrification becomes significant. Hypoxic/anoxic conditions in the open ocean waters of the northern Indian Ocean have not dramatically changed over past decades, but evidence is now emerging that oxygen concentrations are starting to decline, with significant biogeochemical and ecological impacts. The Indian Ocean accounts for ~1/5 of the global oceanic uptake of atmospheric CO₂, with the Arabian Sea as a source of CO₂ to the atmosphere and the southern subtropical gyre as a CO₂ sink. Net CO₂ flux in the Bay of Bengal is uncertain due to sparse sampling. Surface pH values in the Indian Ocean are anomalously low and projected to decline further with negative impacts on calcifying organisms. Dissolved organic carbon (DOC) concentrations in the Indian Ocean tend to be high in near-surface (sub)tropical waters where autotrophic production of DOC exceeds heterotrophic consumption and vertical stability of the water column favors accumulation. In contrast, the highest particulate organic carbon (POC) concentrations in the Indian Ocean are observed in the northwestern part of the basin and the lowest in the southern subtropical gyre, reflecting primary production patterns. POC export flux patterns in the Indian Ocean are similar to the patterns in POC concentration, though carbon flux is also strongly influenced by lithogenic matter content in river-influenced regions like the Bay of Bengal. Observational and modeling research should target improved understanding of northern Indian Ocean OMZ and carbon system variability as such is needed to predict the impacts of anthropogenic influence and global warming on Indian Ocean biogeochemistry and ecosystems.

1
2
3
4
5
6
7
8
9
10
11
12
13
14
15
16
17
18
19
20
21
22
23
24
25
26
27
28
29
30
31
32
33
34
35
36
37
38
39
40
41
42
43
44
45

1. Introduction

1.1 The Northern Indian Ocean oxygen minimum zones (OMZs)

Open ocean Oxygen Minimum Zones (OMZs) occur below the mixed layer of the ocean and are characterized by oxygen concentrations that are low in comparison to surface and deep waters (Dietrich, 1936; Seiwel, 1937; Sverdrup, 1938). Even though mid-water oxygen minimum zones are common features in the ocean, they are typically classified as OMZs only when the lowest minimum oxygen concentrations in the vertical profile drop below certain thresholds (Paulmier et al., 2009). However, due to varying oxygen tolerances of marine organisms, there are multiple definitions for threshold concentrations. Table 1 lays out common definitions, thresholds and impacts of varying definitions of oxygen limitations. A threshold of about 20 $\mu\text{mol/kg}$ is often used to define OMZs because concentrations below this have profound implications for microbes and marine biogeochemical cycles. These oxygen levels are therefore referred to as “microbial hypoxia” (Table 1). The total volume of waters characterized by microbial hypoxia in the global ocean is approximately $15 \times 10^{15} \text{ m}^3$, of which 21% ($3.13 \times 10^{15} \text{ m}^3$) is located in the northern Indian Ocean (Acharya et al., 2016; Garcia et al., 2010). Even though the Indian Ocean OMZ constitutes only 0.23% of the ocean’s volume ($1355 \times 10^{15} \text{ m}^3$) its influence on the cycles of nitrogen, carbon and associated elements is globally significant.

The thickest OMZ in the world is found in the Arabian Sea (e.g., Morrison et al., 1999) where functional anoxia (concentrations $< .05 \mu\text{mol/kg}$, Table 1) occurs in intermediate water (~200-800 m), with profound impact on the nitrogen cycle as a result of denitrification. Very low oxygen concentrations are also found in intermediate water in the Bay of Bengal, but there are important physical and biogeochemical differences between the Arabian Sea and the Bay of Bengal, which have, so far, prevented the development of persistent functional anoxia in the Bay of Bengal OMZ (Figures 1 and 2). Hence in contrast to the Bay of Bengal, the Arabian Sea OMZ is a globally important zone of denitrification (Naqvi et al., 2005), where NO_3^- and NO_2^- are converted to N_2O and N_2 gas, which is then released to the atmosphere. This process of denitrification removes nitrogen containing compounds from the ocean (Figures 1 and 2) and generates N_2O , a prominent greenhouse gas (Ramaswamy et al., 2001, Bange et al. 2001). The Arabian Sea OMZ is most intense in the eastern part of the basin (Figures 1 and 2), with the water column contributing ~10 - 20% of global open-ocean mid-water column denitrification (Codispoti et al., 2001; Rixen et al., 2020; Anju et al., 2022).

Questions remain regarding the relative roles of biological oxygen demand derived from surface organic matter export, versus circulation and ventilation timescales, in maintaining subtle differences in the deep oxygen fields in the Arabian Sea and the Bay of Bengal (Valsala et al., 2009; McCreary et al., 2013; Bopp et al., 2017; Rixen et al., 2020). Recent observational and modeling studies in the Indian Ocean suggest that the OMZs are expanding in response to global warming (Lachkar et al., 2020; Rixen et al., 2020). Perhaps the low nitrogen to phosphorus ratios in the western Bay of Bengal are a harbinger of what is to come (Figure 1). This OMZ expansion is consistent with global modeling studies (Stramma et al., 2008; 2010; Doney, 2010; Figure 3) but uncertainties in global model predictions are large (McCreary et al., 2013; Bopp et

1 al., 2017; Rixen et al., 2020; Kwiatkowski et al., 2020; Schmidt et al., 2020; Schmidt et al.,
2 2021).

3
4 Given the importance of the Indian Ocean OMZs in the global carbon and nitrogen cycles,
5 including the production of radiatively active greenhouse gas, it is essential to understand the
6 biogeochemical variability associated with these regions, their rates of change and the potential
7 implications for global warming.

8 9 **1.2 Role of the Indian Ocean in the global carbon cycle**

10
11 The Indian Ocean plays an important role in the global carbon cycle, yet it remains one of the
12 most poorly sampled ocean regions with respect to inorganic and organic carbon pools and air-
13 sea carbon fluxes (Figures 4, 5 and 6). Estimates suggest that the Indian Ocean accounts for a
14 significant fraction of the global oceanic uptake of atmospheric CO₂ (Takahashi et al., 2002;
15 Sarma et al., 2013; Valsala and Maksyutov, 2013; Sreeush et al., 2018; 2020; de Verneil et al.,
16 2021). This uptake of anthropogenic CO₂ drives a decrease in pH, and indeed, surface pH values
17 in the Indian Ocean are among the lowest of the major ocean basins (Feely et al., 2009; Sreeush
18 et al., 2019). Projected increases in oceanic CO₂ concentrations will lead to further acidification
19 of the Indian Ocean over the coming decades, with potentially severe negative impacts on coral
20 reefs and other calcifying organisms (Hoegh-Guldberg et al., 2007; Doney, 2010).

21
22 Dissolved organic carbon (DOC) is a significant carbon pool in the ocean. As observed
23 elsewhere in the global ocean, DOC concentrations in the Indian Ocean tend to be high in
24 stratified near-surface tropical and subtropical waters where DOC is produced and accumulates,
25 and DOC concentrations are lowest in the deep ocean where heterotrophic consumption of DOC
26 exceeds autotrophic production (Hansell, 2009; Hansell, et al., 2009; Figures 6 and 7).
27 Unsurprisingly, the highest concentrations of DOC are found in the near-surface waters of the
28 central Arabian Sea due to high autotrophic production, and in the northern Bay of Bengal due to
29 the large inputs of fresh water and associated terrigenous DOC flux from rivers (Hansell, 2009;
30 Shah et al., 2018; Figure 6; Data from Hansell and Orellana, 2021). In contrast, particulate
31 organic carbon (POC) concentrations tend to be high in coastal regions of the Indian Ocean
32 where autotrophic production is high, and lowest in the oligotrophic southern subtropical gyre
33 and equatorial waters where autotrophic production is low (Gardner et al., 2006; Figure 8). The
34 highest POC concentrations are found in the western and northern Arabian Sea during the
35 southwest monsoon (SWM) and northeast monsoon (NEM), respectively (Gardner et al., 2006).
36 The spatial and temporal variability in POC export flux in the Indian Ocean is similar to the
37 productivity and POC concentration patterns, consistent with the idea that primary productivity
38 is the main control on the spatial and temporal variability of organic carbon fluxes (Rixen et al.,
39 2019a). However, in regions strongly influenced by river inputs, like the Bay of Bengal, the
40 spatial variability of organic carbon export flux is also strongly influenced by lithogenic matter
41 content, which provides ballast that increases POC sinking rates (Rixen et al., 2019b).

42
43 Understanding and predicting these disparate elements of the carbon cycle and its role in basin
44 acidification in the Indian Ocean is critical for understanding the biogeochemical and ecological
45 evolution of the Indian Ocean under the impact of human activities.

2. Oxygen concentrations and the biogeochemical impacts of the OMZs

The first large ocean-going oceanographic expeditions discovered OMZs in the Indian Ocean between the end of the 19th and the first third of the 20th century (Sewell, 1934; Sewell and Fage, 1948 and references therein). During one of these cruises, the John Murray expedition of 1933 – 34, Gilson (1933) discovered the secondary nitrite maximum of the Arabian Sea, seen as an accumulation of nitrite within the upper part of the OMZ between 200 and 300m depth (Figure 2). Its existence indicates active denitrification (Naqvi, 1991), which in addition to anammox (Dalsgaard et al., 2003; Kuypers et al., 2003) are the main sinks of fixed nitrogen (NH_4^+ , NO_2^- , NO_3^-) in the ocean (Gruber, 2004). Denitrifying microbes use nitrate (NO_3^-) and nitrite (NO_2^-) to fuel heterotrophic respiration in microbially hypoxic waters, in turn reducing these compounds, ultimately, to nitrogen gas (N_2). In contrast, the anammox reaction is carried out by chemoautotrophic microbes that derive energy from the oxidation of NH_4^+ with NO_2^- to produce N_2 in microbially hypoxic waters.

In contrast to fixed nitrogen, N_2 is inaccessible to eukaryotic phytoplankton. Even though there are specific bacterial phytoplankton clades capable of fixing or breaking apart and oxidizing N_2 , the surface ocean is often depleted in fixed nitrogen in comparison to phosphate (Gruber and Sarmiento, 1997). Since phosphate and fixed nitrogen are the primary macro-nutrients required for phytoplankton growth, the intensification of OMZs and the expansion of functional anoxia is assumed to lower marine productivity by favoring denitrification and anammox and thereby the loss of fixed nitrogen in the ocean (Altabet et al., 1995; McElroy, 1983). An interesting feedback is that, over time, reduced productivity and carbon export due to fixed nitrogen loss in turn reduces biological oxygen consumption at depth, such that the expansion of the volume of anoxic waters in the OMZ core can be accompanied by a reduction of the volume of hypoxic waters (Deutsch et al., 2007; Lachkar et al., 2016).

Changes in the coupled marine nitrogen and oxygen cycles also affect the role of the ocean as a sink and/or source of greenhouse gases such as CO_2 and N_2O . The response of the biologically mediated CO_2 uptake of the ocean, referred to as the biological carbon pump (Boyd et al., 2019; Volk and Hoffert, 1985), to environmental changes is difficult to predict (Bopp et al., 2013, De La Rocha and Passow, 2014) because of the multiple processes involved in its functioning (Chakraborty et al., 2018; Boyd et al., 2019). In contrast, the N_2O source function of the ocean is assumed to be directly linked to the expansion and intensity of OMZs, since N_2O is an intermediate product formed during denitrification (Bange et al., 2001; Fuhrman and Capone, 1991).

Even though denitrification and anammox occur at microbially hypoxic levels of oxygen (concentrations $< 20 \mu\text{mol/kg}$; Table 1), their impact on the nitrogen cycle becomes significant only with the occurrence of functional anoxia (concentrations $< .05 \mu\text{mol/kg}$; Table 1). At such low oxygen concentrations, the reduction of nitrite to N_2 outcompetes the re-oxidation of nitrite to nitrate, leading to net loss of fixed nitrogen (Bristow et al., 2017; Gaye et al., 2013). The re-oxidation of nitrite to nitrate prevents, in turn, the loss of fixed nitrogen and the formation of the secondary nitrite maximum at higher oxygen concentrations within the OMZ. In contrast to the Bay of Bengal OMZ, which is on the verge of becoming functionally anoxic (Bristow et al.,

1 2017), functional anoxia is wide spread in the Arabian Sea OMZ as indicated by the extent of the
2 secondary nitrate maximum (Naqvi, 1991; Rixen et al., 2014; Figure 2).

3 4 **2.1 Oxygen distributions, sources and sinks**

5
6 Low oxygen conditions in the water column are usually associated with slow ventilation and
7 high biological oxygen demand. OMZs are hence found in productive but poorly ventilated
8 shadow zones of the subtropical oceans, where subsurface water masses recirculate beneath a
9 shallow mixed-layer with minimal direct advective or mixing connection to the surface ocean
10 (Luyten et al., 1983). In these domains, the residence time below the thermocline is at a
11 maximum and oxygen is slowly supplied mainly through isopycnal (horizontal) mixing
12 processes (Gnanadesikan et al., 2012; Levy et al., 2021). Moreover, the strong and localized
13 subsurface biological oxygen consumption in OMZs generates strong spatial gradients in oxygen
14 at their edges, making mixing central to the oxygen balance. The Arabian Sea OMZ is not a
15 classical shadow zone due to the northern boundary of the Asian subcontinent, but diapycnal and
16 isopycnal mixing are likely the main oxygen sources balancing strong biological depletion in the
17 core of the OMZ, in roughly equal proportions (Resplandy et al., 2012). Model simulations
18 suggest that without oxygen supplied by eddy mixing, the volume of the Arabian Sea OMZ
19 would double (Lachkar et al., 2016).

20
21 In addition to mixing processes in the core of the OMZ, the inflow of oxygen-enriched Indian
22 Ocean Central Water and Persian Gulf Water are assumed to be the main physical oxygen supply
23 mechanism to the edges of the OMZ in the Arabian Sea (Lachkar et al., 2019; McCreary et al.,
24 2013; Resplandy et al., 2012; Sen Gupta and Naqvi, 1984; Swallow, 1984). Indian Ocean Central
25 Water forms through convective mixing as Subantarctic Mode Water in the southern Indian
26 Ocean and is advected northward into the OMZs in both the Arabian Sea and Bay of Bengal
27 (Fine, 1993; McCartney, 1979; Sverdrup et al., 1942). Oxygen-enriched Persian Gulf Water is
28 introduced into the Arabian Sea OMZ after its outflow from the Persian Gulf (Rixen et al., 2005;
29 Schmidt et al., 2020; Schmidt et al., 2021; Tchernia, 1980; Lachkar et al. 2019). The negative
30 water balance of the Persian Gulf drives this localized deep-water formation by increasing the
31 salinity and hence the density of Persian Gulf Water.

32
33 The oxygen-poor Arabian Sea intermediate water, in turn, flows into the Bay of Bengal OMZ
34 (Figure 1), where high freshwater inputs from rivers and monsoon rainfall (Figure 5) reduce the
35 vertical oxygen supply by increasing stratification in the surface layers (Rixen et al., 2020).
36 However, in comparison to the Arabian Sea, lower biomass (Figure 8), productivity and a
37 stronger ballast effect prevent development of functional anoxia in the Bay of Bengal OMZ by
38 keeping biological oxygen consumption lower (Al Azhar et al., 2017; Rao et al., 1994; Rixen et
39 al., 2019b). Ballast minerals, which are supplied from land via rivers or as dust, accelerate the
40 sinking of particles, lowering the residence time of exported organic matter in the water column
41 and thereby its decomposition in the OMZ (Haake and Ittekkot, 1990; Ramaswamy et al., 1991).
42 It should be noted, however, that the ballast effect appears to be important primarily in the
43 northern Bay of Bengal (Ittekkot et al., 1991), which suggests that the primary cause of the higher
44 oxygen concentrations further south in the Bay of Bengal is the lower biomass and productivity
45 that results in reduced export and a lower biological oxygen demand. In contrast to the Bay of
46 Bengal, a weak ballast effect and a higher biological production (Figure 8) sustain a higher

1 biological oxygen consumption at intermediate depths in the Arabian Sea. This enhanced
2 biological oxygen consumption balances the higher physical oxygen supply in the Arabian Sea
3 and explains the more intense OMZ (Rixen et al., 2019a).

4
5 Contrary to expectations, the Arabian Sea OMZ is more intense in the eastern part of the basin
6 and less intense in the western parts of the basin where productivity is highest (Antoine and
7 Morel, 1996; Naqvi, 1991; McCreary et al., 2013). The thickest part of the OMZ is in the
8 northeastern Arabian Sea (Sarma et al., 2020). Multiple factors are presumed to cause this
9 asymmetry. The inflow of Indian Ocean Central Water and Persian Gulf Water ventilates the
10 western Arabian Sea preferentially, and is assumed to cause this eastward displacement
11 (Resplandy et al., 2012; McCreary et al., 2013; Rixen et al., 2014). Additionally, the seasonal
12 monsoon-driven reversal of the surface ocean circulation leads to intense vertical eddy mixing in
13 the western Arabian Sea causing an eastward shift of the upper OMZ relative to the region of
14 highest productivity (Resplandy et al., 2012; McCreary et al., 2013; Lachkar et al., 2016).
15 Similarly, the eastward shift of the OMZ has been attributed to weak mixing and high
16 penetration time of intermediate water masses in the northeastern Arabian Sea, with the
17 additional influence of organic matter transport from the shelf region that enhances biological
18 oxygen demand (Sarma et al., 2020).

21 **2.2 Biogeochemical impacts of the northern Indian Ocean OMZs**

22
23 The Arabian Sea and the Bay of Bengal collectively contain ~59% of the Earth's marine
24 sediments exposed to hypoxia (Helly and Levin, 2004). Denitrification within sediments (benthic
25 denitrification) underlying functionally anoxic conditions in the water column, is the largest sink
26 for fixed nitrogen in the ocean (Gruber, 2004; DeVries et al., 2013). However, estimates of the
27 relative rates of benthic and water column denitrification are still fraught with large uncertainties
28 on global as well as regional scales. Hence, the role of the Arabian Sea as a sink of fixed
29 nitrogen is difficult to quantify. Although denitrification in the Arabian Sea has been much more
30 intensively studied than in the Bay of Bengal, estimates of benthic and water column
31 denitrification in the Arabian Sea still encompass a wide range with means of 3.9 ± 2.9 Tg N
32 year⁻¹ and 17 ± 16 Tg N year⁻¹, respectively (Bange et al., 2000; Bristow et al., 2017; Deuser et
33 al., 1978; Gaye et al., 2013; Howell et al., 1997; Naqvi et al., 1982; Somasundar et al., 1990).
34 Considering global mean estimates of benthic and water-column denitrification of 183 ± 118 Tg
35 N year⁻¹ and 155 ± 116 Tg N year⁻¹ (Eugster and Gruber, 2012; Gruber, 2004; Somes et al.,
36 2013), on average the Arabian Sea comprises approximately 2% and 11% of the global mean
37 benthic and water column denitrification, respectively. It should be noted, however, that more
38 recent data indicate that benthic denitrification at the Pakistan continental margin alone could be
39 up to 10.5 Tg N year⁻¹ (Schwartz et al., 2009; Somes et al., 2013), greatly exceeding the
40 previously estimated benthic denitrification of 3.9 ± 2.9 Tg N year⁻¹ for the entire Arabian Sea.
41 Moreover, the most recent observations suggest the northeastern Arabian Sea has a water column
42 denitrification rate of 25.3 ± 7.0 Tg N yr⁻¹ (Anju et al., 2022). These estimates suggest that the
43 Arabian Sea comprises at least 6% and 16% of the global mean benthic and water column
44 denitrification, respectively.

1 The volume of hypoxic waters and rate of denitrification in the Arabian Sea strongly increase in
2 response to enhanced monsoon winds (Lachkar et al., 2018). Stronger winds intensify the
3 upwelling, increasing biological productivity and respiration in excess of the increase in wind-
4 driven ventilation and are also responsible for the deepening of the OMZ. However, as discussed
5 above, increases in denitrification have the potential to reduce biological productivity through
6 nitrogen removal, and hence the efficiency of the biological pump of carbon, at the basin scale
7 (and beyond) on timescales of decades to centuries (Lachkar et al., 2018; Canfield et al., 2019;
8 McElroy, 1983). Therefore, an expansion of Indian Ocean OMZs can affect the large-scale
9 biogeochemical cycles of nitrogen and carbon and contribute to climate variations over long
10 timescales (Altabet et al., 2002; Gaye et al., 2018). The extent of this control depends on the
11 magnitude of the nitrogen removal and the importance of concurrent stabilizing negative
12 feedbacks, including the feedback of reduced productivity on biological oxygen demand and the
13 tight coupling between denitrification and N₂ fixation downstream of OMZs (Deutsch et al.,
14 2007, Gruber and Galloway, 2008). If the excess in phosphorus relative to nitrogen supports
15 local nitrogen fixation within the Indian Ocean basin, the timescales for feedbacks with
16 denitrification could be much shorter than the timescale of the global ocean circulation.

17 18 **2.3 Recent (decadal) changes in oxygen concentrations**

19
20 Early reports on the occurrence of coastal hydrogen sulfide in the north-eastern Arabian Sea and
21 off Oman at Ras-al-Hadd (Carruthers et al., 1959; Ivanenkov and Rozanov, 1966) indicate that
22 the Arabian Sea OMZ was more intense in the past because the emergence of hydrogen sulfide
23 indicates the transition from functional anoxia (oxygen < .05 μmol/kg) towards anoxic (zero
24 oxygen) conditions (Table 1). These are the only reports of the occurrence of hydrogen sulfide in
25 the Arabian Sea except for Naqvi et al. (2000), who discovered an anoxic event that developed
26 along the western Indian coast off Mumbai in the late summer of 1999. Such strong events do
27 not develop every year (Gupta et al., 2016; Sudheesh et al., 2016), but their appearance shows
28 that the spreading of oxygen-depleted zones in coastal regions is a global phenomenon that does
29 not spare the Indian shelf (Altieri et al., 2017; Diaz and Rosenberg, 2008; Diaz et al., 2019).
30 However, contrary to this prevailing understanding, Gupta et al. (2021) argue that the hypoxic-
31 anoxic zone along the west coast of India is formed through a natural process, i.e., upwelling of
32 deoxygenated waters during the summer monsoon, and that the persistence and extent of this
33 coastal oxygen deficiency depend on the degree of deoxygenation of source waters for the
34 upwelling. Moreover, the volume of anoxic waters is strongly modulated by the Indian Ocean
35 Dipole (IOD), with positive IOD events preventing anoxia due to wind-forced downwelling
36 coastal Kelvin waves propagating along the west coast of India (Vallivattathillam et al., 2017).

37
38 In contrast to these shelf processes, there is only a weak decadal decline in dissolved oxygen
39 concentrations in the OMZs of the Arabian Sea and the Bay of Bengal in comparison to OMZs
40 of the South Atlantic Ocean and the Pacific Ocean (Ito et al., 2017; Naqvi, 2019; Schmidtko et
41 al., 2017; Stramma et al., 2008). The analysis of all oxygen data available from the Arabian Sea
42 between 1959 and 2004 by Banse et al. (2014) ascribes this modest change to opposing regional
43 trends within the Arabian Sea, where oxygen concentrations increased in the southern part of the
44 Arabian Sea and declined in the central Arabian Sea. In contrast, Sarma et al. (2018) ascribe the
45 modest change in oxygen levels in the Bay of Bengal to the influence of anticyclonic eddies in
46 that precluded the OMZ from intensifying. Follow-up studies report decreasing oxygen

1 concentrations in the western and northern Arabian Sea (Piontkovski and Al-Oufi, 2015; Queste
2 et al., 2018). In the northern Arabian Sea, dissolved oxygen concentrations in the surface mixed
3 layer largely reflect the decreasing trend seen in the OMZ, as indicated by a compilation of
4 dissolved oxygen data covering the period from the 1960s to 2010 (Gomes et al., 2014). In
5 response to this deoxygenation, the secondary nitrite maximum expanded southward and
6 westward in the early 1990s (Rixen et al., 2014). Perhaps in response to changing oxygen
7 concentrations, the planktonic community structure has changed as shown by the development
8 and now regular occurrence of large *Noctiluca* winter blooms since the 2000s in the Arabian Sea
9 (Hood et al, 2022 this volume; Gomes et al, 2014; Goes and Gomes, 2016; Goes et al., 2020). It
10 should be noted, however, that it has been shown that *Noctiluca* blooms occur in oxic conditions,
11 and that both natural and anthropogenic processes appear to have contributed to the development
12 of the massive blooms in the northeastern Arabian Sea (Sarma et al., 2018; Sridevi and Sarma,
13 2022). Numerical model results suggest that reduced ventilation caused by a reduced inflow of
14 Persian Gulf Water in response to warming, combined with reduced solubility of oxygen in
15 surface water of the Persian Gulf, may have contributed to these developments (Lachkar et al.,
16 2019). In addition to changes in the Gulf outflow, recent numerical model results also attribute
17 decreasing oxygen concentrations in the northern Arabian Sea to reduced local ventilation due to
18 global warming-induced increases in stratification and weakening of winter convective mixing
19 (Lachkar et al., 2020).

20
21 Nonetheless, widespread and or more frequent outbreaks of hydrogen sulfide as seen in the
22 upwelling systems off Peru (Schunck et al., 2013) and Namibia (Weeks et al., 2002) have not so
23 far been reported in the northern Indian Ocean during the last 50 years. This finding implies that
24 the interplay between physical oxygen supply and the biological oxygen consumption has
25 prevented the development of persistent anoxia (zero oxygen) in the Arabian Sea and functional
26 anoxia (oxygen < .05 μM) in the Bay of Bengal OMZ (Rixen et al., 2020).

27 28 **2.4 Future changes in oxygen concentrations**

29
30 There is high uncertainty in the future evolution of the Arabian Sea OMZ, and of all major
31 OMZs, projected by Earth System models by year 2100 (Bopp et al., 2013, Cabré et al. 2015,
32 Kwiatkowski et al., 2020; Rixen et al., 2020). The uncertainty largely arises from differences
33 among models in the magnitude and timing of changes in ventilation and biological oxygen
34 demand and how strongly they offset each other (Resplandy, 2018). Both processes are strongly
35 influenced by model resolution and are thus challenging to simulate at the centennial scale. It is
36 projected that OMZs may either shrink or expand under projected climate change, depending on
37 the efficiency of mixing (Duteil and Oschlies, 2011, Bahl et al., 2019, Lévy et al., 2021). As
38 discussed above, this uncertainty is particularly large in the northern Indian Ocean where global
39 forecast models generally fail to reproduce the current oxygen concentrations and distributions
40 (McCreary et al., 2013; Rixen et al., 2020; Schimdt et al., 2021). This failure, and the
41 uncertainty in future projections, may also be related to the lack of consideration of the role of
42 cross-shelf transport of organic matter in Earth System models, which is a process that is known
43 to contribute to the development of the OMZs in both the Arabian Sea and Bay of Bengal (Sarma
44 et al., 2020; Udaya Bhaskar et al., 2021).

45 46 **3. Carbon concentrations and fluxes**

1
2 The earliest CO₂, pH and POC measurements in the Indian Ocean date back to the International
3 Indian Ocean Expedition in the early 1960s (Figure 4; e.g., Newell, 1969; Berhman, 1981).
4 Carbonate system measurements were also made in the Indian Ocean under the Geochemical
5 Ocean Section Study (GEOSECS) in the 1970s (Moore, 1984), the Joint Global Ocean Flux
6 Study (JGOFS; Fasham, 2003; see also
7 https://en.wikipedia.org/wiki/Joint_Global_Ocean_Flux_Study) and the World Ocean
8 Circulation Experiment (WOCE) in the 1990s (Woods, 1985). Subsequently in the first decade
9 of the 21st century CLIVAR Repeat Hydrography project started (Gould et al., 2013), and
10 carbonate system measurements continue through the present under the ongoing GO-SHIP
11 program (Talley et al., 2017; see also <https://www.go-ship.org/About.html>) and the Second
12 International Indian Ocean Expedition (IIOE-2; Hood et al., 2015). In addition to these major
13 international efforts, there have been numerous national expeditions and programs that have
14 contributed to the current inventory of carbonate system measurements in the Indian Ocean. For
15 example, time-series observations of pH and pCO₂ are being made in the coastal waters of India
16 revealing recent trends (Sarma et al., 2021). There is also now a mooring in the central Bay of
17 Bengal (Figure 4) that has been collecting continuous CO₂ and pH measurements since
18 November, 2013 (see <https://www.pmel.noxxaa.gov/co2/story/BOBOA>).
19

20 In contrast, the history of DOC measurements in the Indian Ocean dates back only to the early
21 1990s when it was discovered (thanks to advances in measurement methods that achieved ~ 1
22 µmol/kg precision sufficient to reveal DOC variability over space and time) that DOC
23 concentrations are more dynamic than previously thought (Hansell, 2009). The timing of this
24 discovery coincided with the onset of the JGOFS Arabian Sea Process Study when some of the
25 earliest “modern” Indian Ocean DOC measurements were made. Subsequently, DOC
26 concentration measurements were made in the Indian Ocean under the US CLIVAR Repeat
27 Hydrography project and they continue under the ongoing GO-SHIP program and through
28 national expeditions. DOC isotopes measurements are also now being made in the northern
29 Indian Ocean to provide insight into DOC sources (Rao and Sarma, 2022).
30

31 **3.1 Inorganic carbon distributions and fluxes**

32

33 The Indian Ocean accounts for ~20% of the global oceanic uptake of atmospheric CO₂
34 (Takahashi et al., 2002). The Arabian Sea is a source of CO₂ to the atmosphere due to elevated
35 pCO₂ within the Southwest Monsoon (SWM)-driven upwelling (Figure 4; see also Takahashi et
36 al., 2009; 2014; Valsala and Maksyutov, 2010; 2013; de Verneil et al., 2021). North of 14°S the
37 Indian Ocean loses CO₂ at a rate of 0.12 – 0.16 PgC/yr (Takahashi et al., 2002; 2009; 2014; de
38 Verneil et al., 2021). The most intense air-sea CO₂ exchange occurs during the SWM where
39 outgassing rates reach ~6 molC/m²/yr in the upwelling regions off Oman and Somalia, but the
40 entire Arabian Sea contributes CO₂ to the atmosphere (Valsala and Murtugudde, 2015; Sreesh
41 et al., 2018; 2020; de Verneil et al., 2021).
42

43 Time series measurements have shown that the rates of increase in DIC and pCO₂ per decade are
44 consistent with global trends in the southwestern coastal Bay of Bengal, whereas rates in the
45 northwestern coastal Bay of Bengal have been observed to be 3 to 5 times higher than the global
46 trends (Sarma et al., 2015a). Thus, the northwestern Bay of Bengal, which was previously

1 considered to be a significant sink for atmospheric CO₂, now seems to have become a source of
2 CO₂ to the atmosphere. Variability in CO₂ fluxes in the northwestern shelf region of the Bay of
3 Bengal depends on the river discharge characteristics and the East India Coastal Current that
4 distributes this water along the coast (Sarma et al., 2012). Nonetheless, it is still uncertain
5 whether the entire Bay of Bengal is a net CO₂ source or sink due to the high levels of variability
6 combined with sparse spatial and temporal sampling (Figure 4; Bates et al., 2006). South of 14°S
7 the Indian Ocean appears to be a strong net CO₂ sink (-0.44 PgC/yr in the band 14°S-50°S;
8 Figure 4). The solubility pump (CO₂ dissolution and its physical mixing and transport) and the
9 biological pump (biologically mediated processes that export carbon) contribute equally to the
10 CO₂ sink in the south Indian Ocean region (Valsala et al., 2012). Cold temperatures increase CO₂
11 solubility at higher latitudes and subduction in the subtropical front can transport this CO₂ into
12 the ocean interior, but there is also evidence that chemical and biological factors are important,
13 e.g., potential iron fertilization that facilitates particulate carbon export in the southern
14 hemisphere of the Indian Ocean (Piketh et al., 2000).

15
16 In addition, the IOD leads to a substantial sea-to-air CO₂ flux variability in the southeastern
17 tropical Indian Ocean over a broad region (70–105°E, 0–20°S), with the most intense effects
18 manifesting near the coast of Java-Sumatra due to the impacts on upwelling dynamics and
19 associated westward propagating anomalies. The sea-to-air CO₂ fluxes, surface ocean partial
20 pressure of CO₂ (pCO₂), the concentration of dissolved inorganic carbon (DIC), and ocean
21 alkalinity (ALK) range as much as ±1.0 mole m⁻² yr⁻¹, ±20 µatm, ±35 µmole kg⁻¹, and ±22
22 µmole kg⁻¹, respectively, within 80–105°E, 0–10°S due to the IOD. The DIC and ALK are
23 significant drivers of pCO₂ variability associated with IOD (Valsala et al., 2020).

24
25 Synthesis of the seasonal, annual and interannual air-sea CO₂ fluxes based on both models
26 (ocean, atmospheric inversions) and observations (Takahashi et al., 2009) reveals that the net
27 sea-air CO₂ uptake estimated from observations (-0.24 PgC/yr) is consistent with uptake derived
28 from models (-0.37 PgC/yr), given the uncertainties (Sarma et al., 2013). However, some models
29 overestimate flux in the Bay of Bengal and underestimate flux in the Arabian Sea / northwestern
30 Indian Ocean (Sarma et al., 2013). These offsets are likely due to the models being inadequately
31 constrained by CO₂ observations. There are fewer observations in the Indian Ocean (especially
32 north of 20°S) compared to other oceans in recent years (Figure 4; Bakker et al., 2014, see also
33 www.socat.info). More observations of ocean DIC concentrations and carbon flux are needed in
34 the Indian Ocean to constrain the models and reduce uncertainties in the fluxes. Toward this
35 goal, Valsala et al. (2021) has recently done observing system simulation experiments for Indian
36 Ocean pCO₂ arrays and recommended deployment of additional moorings at suitable locations to
37 monitor and better constrain the Indian Ocean air-sea CO₂ fluxes. A few key ship-of-opportunity
38 routes for underway pCO₂ sampling in the Indian Ocean are also recommended in their study.

39 40 **3.2 Spatial and temporal variability in pH**

41
42 Uptake of anthropogenic CO₂ by the ocean results in fundamental changes in seawater chemistry
43 that can have significant impacts on ocean ecosystems (Doney et al., 2010; Gattuso and Hansson,
44 2011). Intergovernmental Panel on Climate Change (IPCC) business-as-usual emission scenarios
45 indicate that atmospheric CO₂ levels will reach 800 ppm near the end of this century (Feely et
46 al., 2009). The associated increase in oceanic CO₂ concentrations will lead to acidification (lower

1 pH) of the Indian Ocean over the coming decades, with potential severe negative impacts on
2 coral reefs and other calcifying organisms (Doney, 2010; IPCC, 2019). In 1995, the surface pH
3 values for the northern (20°E-120°E, 0°-24.5°N) and southern (20°E-120°E, 0°-40°S) Indian
4 Oceans were 8.068 +/- 0.03 and 8.092 +/- 0.03, respectively, which is the lowest of the major
5 ocean basins (Feely et al., 2009). It is not entirely clear why surface pH values are so low in the
6 Indian Ocean (Takahashi et al., 2014). Increases in sulphate and nitrogen aerosol loadings over
7 the Bay of Bengal from the Indo-Gangetic Plain and Southeast Asia may be mainly responsible
8 for the increased acidity in the northwestern Bay of Bengal in recent years (Sarma et al., 2015a).
9 Reduced Godavari River discharge together with a positive IOD event have also been shown to
10 contribute to enhanced acidification and pCO₂ levels in the coastal waters in the western Bay of
11 Bengal (Sarma et al., 2015b). A study from the eastern Bay of Bengal indicates a decline in pH
12 of 0.2 from 1994 to 2012 (Rashid et al., 2013), which is considerably faster than the global
13 decline of 0.1 over the last century (IPCC 2007). Upwelling of low pH subsurface waters in the
14 Arabian Sea results in low surface pH (<7.9) during the SWM (Takahashi et al., 2014). Sreesh
15 et al. (2019) estimated that in addition to the anthropogenic causes, ocean warming exacerbates
16 acidification in the western Arabian Sea by an additional 16%. Chakraborty et al. (2021) studied
17 the seasonal drivers of surface ocean pH in the Arabian Sea and Bay of Bengal and found that
18 DIC and SST make complementary contributions to the seasonal cycle in pH. Tarique et al.
19 (2021) reported the first time series of Arabian Sea pH from proxy records of Boron Isotopes
20 from 1990 to 2013. Their investigation reveals that physical oceanographic processes, for
21 example, upwelling, downwelling and convective mixing modulated by El Niño-Southern
22 Oscillation (ENSO), largely control surface pH variability and mask expected long-term ocean
23 acidification trends resulting from anthropogenic CO₂ rise. An increase in pH has been observed
24 in the eastern and southern Bay of Bengal during all seasons associated with warming and a
25 decrease in salinity (Sridevi and Sarma, 2021). In contrast, a decrease in pH (-0.001 yr⁻¹) and a
26 pCO₂ increase (+0.1 to +0.7 μatm yr⁻¹) has been observed in the western and northern Bay of
27 Bengal during winter and spring seasons due to deposition of atmospheric pollutants (Sridevi and
28 Sarma, 2021). These studies suggests that increases in freshwater input due to melting of
29 Himalayan ice cover and deposition of atmospheric pollutants are dominant controlling factors
30 on surface ocean pH and pCO₂ in the Bay of Bengal between 1998 and 2015, and this region is
31 acting as a stronger sink for the atmospheric CO₂ in the present than in the past two decades
32 (Sarma et al., 2021; Sridevi and Sarma, 2021).

33
34 The susceptibility of the Indian Ocean coral communities to warming has been revealed by the
35 large-scale coral bleaching events of 1998, 2005, 2011 as well as between 2014 and 2017 caused
36 by high SST (McClanahan et al., 2007; Moore et al., 2012, Obura et al. 2017, Cerutti et al.
37 2020). Ocean acidification has the potential to exacerbate these negative impacts on coral reef
38 ecosystems. For example, the 1998 bleaching event altered the age distribution of commercially
39 harvested fish (Graham et al. 2007). Because of the combined effects of acidification, human
40 development and global warming, coral reef ecosystems may be at greater risk than previously
41 thought (Hoegh-Guldberg et al., 2007; IPCC, 2019). Moreover, some commercially fished
42 species (e.g., shelled mollusks) are directly vulnerable to ocean acidification (Hoegh-Guldberg et
43 al., 2014). A study off Somalia suggests that human-induced ocean acidification reduced the rate
44 at which foraminifera calcify, resulting in lighter shells (de Moel et al., 2009). Due to the effects
45 of acidification on calcifying pteropods, which are preyed on by many higher trophic level

1 organisms, the Southern Ocean sector of the Indian Ocean could experience major disruptions in
2 pelagic food webs (Bednarsek et al., 2012).

3
4 In addition to the direct impacts of acidification, increasing CO₂ in the upper ocean could lead to
5 increased primary productivity for some species (e.g., diazotrophic cyanobacteria; Hutchins et
6 al., 2007), altering rates of nitrogen fixation and therefore the biogeochemistry of particulate
7 organic matter formation and remineralization. Declines in pH also shift the chemical
8 equilibrium from ammonia (NH₃) to ammonium (NH₄⁺), which could alter key biogeochemical
9 processes such as nitrogen assimilation by phytoplankton and microbial nitrification (Gattuso
10 and Hansson, 2011).

11 **3.3 Large scale DOC and POC distribution and fluxes**

12
13
14 Near-surface (< 50 meters) DOC concentrations in the Indian Ocean vary between ~50 and 80
15 μmolC/kg with the lowest values occurring south of 40° S (Hansell, 2009; Hansell et al., 2009;
16 Figures 6, 7). In general, near-surface concentrations of DOC are positively correlated with
17 temperature and, to a lesser extent, they are negatively correlated with nutrient concentrations.
18 The positive correlation with temperature happens because warm, low-latitude waters tend to be
19 more strongly stratified, and there is reduced vertical mixing. As a result, DOC concentrations
20 increase in these waters even though there are low rates of net DOC production because the DOC
21 is not mixed away (Hansell, 2009). As a result, near-surface DOC concentrations in the Indian
22 Ocean tend to be highest (> 70 μmolC/kg) in tropical and subtropical waters (Hansell, 2009;
23 Hansell et al., 2009; Figure 7). These patterns are also found in the Atlantic and Pacific
24 (Hansell, 2009; Hansell et al., 2009).

25
26 Near-surface DOC concentrations tend to be inversely correlated with nitrate, silicate and
27 phosphate concentrations because, when these nutrients are consumed, DOC is produced
28 (Hansell, 2009). Thus, a negative correlation is also observed between DOC and nitrate and
29 phosphate concentrations in the deep waters (> 500 meters) of the Indian Ocean where DOC
30 concentrations decline to < 50 μmolC/kg (Figure 7) and nitrate and phosphate concentrations are
31 substantially enriched. However, these correlations are not observed between DOC and silicate
32 concentrations because in deep waters of the Indian Ocean there are large gradients in silicate
33 that are associated with very little change in DOC (Hansell, 2009).

34
35 As in the Pacific and Atlantic, the lowest DOC concentrations in the Indian Ocean (40 - 42
36 μmol/kg at 3000 meters) are found below 1000 meters depth (Figure 7; Figure 2 in Hansell, et
37 al., 2009). Global observations show that DOC concentrations below 1000 meters depth in the
38 Indian Ocean are comparable to those in the Atlantic and significantly higher than deep DOC
39 concentrations in the Pacific (< 40 μmolC/kg at 3000 meters; Hansell et al., 2009). DOC
40 concentrations decline below the euphotic zone because heterotrophic consumption exceeds
41 autotrophic production (Hansell et al., 2009). Presumably, a significant fraction of the DOC
42 below 1000 meters in the Indian Ocean is very old (> 4000 years) and refractory (resistant to
43 bacterial consumption) as has been shown to be the case in the Atlantic and Pacific (Bercovici et
44 al., 2018).

1 As observed elsewhere in the global ocean, satellite-estimated near-surface POC concentrations
2 are elevated in coastal regions of the Indian Ocean with values often exceeding 120 mgC/m^3 (= $10 \text{ } \mu\text{molC/kg}$; Figure 8; Gardner et al., 2006). The highest POC concentrations in the Indian
3 Ocean are observed in the northwestern part of the basin in the Arabian Sea and off of the coast
4 of Somalia with values estimated to be greater than 96 mgC/m^3 (= $8 \text{ } \mu\text{molC/kg}$) extending well
5 into the open ocean during the NEM (Figure 8). These high POC values are associated with high
6 chlorophyll concentrations, although chlorophyll itself only accounts for $> .6\%$ of the POC and
7 presumably the remainder is cellular and detrital material (Gardner et al., 2006). Note that C:Chl
8 ratios range from ~ 15 - 158 by weight (Sathyendrenath et al, 2009). Elevated POC concentrations
9 ($> 72 \text{ mgC/m}^3 = 6 \text{ } \mu\text{molC/kg}$) are also observed in the Indonesian Throughflow region
10 (particularly during the Southeast Monsoon, SEM) and off of southern Africa over the Agulhas
11 Bank, and in the Agulhas Current and its retroflexion, again associated with high chlorophyll
12 concentrations ($> .4\%$ of POC; Figure 8, Gardner et al., 2006). The lowest POC concentrations
13 in the Indian Ocean are observed between 40° S and 10° N in the oligotrophic southern
14 subtropical gyre and equatorial waters where primary production is very low (Gardner et al.,
15 2006; Figure 8; see below).
16

17
18 Unsurprisingly, the spatial and temporal variability in POC export flux in the Indian Ocean is
19 similar to the above mentioned patterns in POC and chlorophyll concentration, consistent with
20 primary production as the main control on the spatial and temporal variability of organic carbon
21 fluxes (Rixen et al., 2019a). However, as discussed above, in river-influenced regions like the
22 Bay of Bengal, the spatial variability of organic carbon flux is also strongly influenced by
23 lithogenic matter content. Rixen et al. (2019b) estimate that lithogenic matter content enhances
24 organic carbon flux rates on average by 45% and by up to 62% in river-influenced regions of the
25 Indian Ocean. This strong ballast effect explains why organic carbon fluxes are lower in the
26 highly productive western Arabian Sea than they are in the relatively unproductive southern Java
27 Sea. This explanation appears to be broadly consistent with the earlier global estimates of
28 organic carbon burial and sediment accumulation rates calculated by Janke (1996; Figure 9),
29 indicating that both are elevated in the coastal and northern regions of the Arabian Sea where
30 rates of primary production are very high, but river influence is small. In contrast, both organic
31 carbon burial and sediment accumulation rates are elevated over a much larger area in the Bay of
32 Bengal where primary production is lower, but river influence is large (Janke, 1996; Figure 9).
33

34 **3.4 Regional DOC and POC distributions and fluxes**

35 **3.4.1 Arabian Sea**

36
37
38 DOC in the surface ocean is a short-term reservoir for carbon, expanding and contracting
39 seasonally. In the Arabian Sea the highest near-surface (< 50 meters) DOC concentrations (80 -
40 $100 \text{ } \mu\text{molC/kg}$) are observed near the coast when upwelling is not active. During the SWM,
41 upwelling results in lowered near-surface DOC concentrations along the western side of the
42 basin, i.e., DOC concentrations increase seaward from $< 70 \text{ } \mu\text{molC/kg}$ near the coast to > 80
43 $\text{ } \mu\text{molC/kg}$ in the central Arabian Sea. In the open ocean, the highest surface DOC concentrations
44 (80 - $95 \text{ } \mu\text{molC/kg}$) are observed during the Northeast Monsoon (NEM) and they remain high
45 through mid SWM. The lowest open ocean near-surface DOC concentrations (65 - $75 \text{ } \mu\text{molC/kg}$)

1 are observed during late SWM and during the Fall Intermonsoon (Hansell and Peltzer, 1998;
2 Hansell, 2009).

3
4 The seasonal accumulation of DOC north of 15°N in the Arabian Sea happens mostly during the
5 NEM, and it has been estimated to be equivalent to 6-8% of annual primary production and 80%
6 of net community production. In contrast, net DOC production is very small during the SWM
7 (Hansell and Peltzer, 1998).

8
9 In the vertical, DOC concentrations decrease to values of <55 $\mu\text{molC/kg}$ at the top of the OMZ
10 (~100 meters). Vertical layering is also observed in DOC concentrations in the Arabian Sea and
11 is associated with vertical layering of the water masses, with Persian Gulf Water producing a
12 clear signal of elevated DOC. DOC concentrations below 500 meters are low (<50 $\mu\text{molC/kg}$)
13 and relatively uniform across the basin and there appears to be little impact of the OMZ on DOC
14 concentrations (Hansell and Peltzer, 1998; Hansell, 2009).

15
16 Consistent with satellite estimates (Gardner et al., 2006), in situ measurements of near surface (0
17 - 150 meters) POC concentrations in the Arabian Sea are generally high near the coast of Oman
18 and decrease offshore throughout the year with concentrations often exceeding 12.5 $\mu\text{molC/kg}$
19 (Gunderson et al., 1998; Figure 10). The spatial distributions are always patchy due to the
20 influence of mesoscale eddies and jets. Seasonal variations in POC concentrations in the upper
21 150 m can be the same order of magnitude as basin-wide spatial variations and these
22 concentrations are strongly influenced by nutrient availability and mixing (Gunderson et al.,
23 1998). POC and chlorophyll concentrations are clearly correlated (Figures 10 and 11), indicating
24 that variability in phytoplankton production drives much of the observed POC variations
25 (Gunderson et al., 1998; Gardner et al., 2006). Subsurface POC and chlorophyll maxima are also
26 observed, particularly offshore and during the intermonsoon periods with the latter generally
27 deeper and more pronounced, as observed elsewhere (e.g., Fennel and Boss, 2003; see also
28 review by Cullen, 2015). Interestingly, when POC and chlorophyll concentrations are vertically
29 integrated the values can be higher during the spring intermonsoon than during the SWM
30 because of the strong subsurface POC and chlorophyll maxima that develop during the spring
31 intermonsoon (Gunderson, et al., 1998).

32
33 In the Arabian Sea, POC export normalized to 2000 meters ranges from < 6 to > 22 $\text{mgC m}^{-2} \text{d}^{-1}$
34 (equal to < 0.5 to > 1.8 $\text{mmolC m}^{-2} \text{d}^{-1}$) depending upon location and season (Rixen et al., 2019;
35 Honjo et al., 1999). In contrast, POC export from the base of the euphotic zone in the western
36 Arabian Sea estimated from the satellite-derived net primary production data and export fluxes
37 calculated with a model give 258.3 and 335.7 $\text{mgC m}^{-2} \text{d}^{-1}$ (equal to 21.5 and 27.9 $\text{mmolC m}^{-2} \text{d}^{-1}$
38 ¹), respectively (Sreeush et al., 2018), suggesting dramatic declines in export at depth compared
39 to the surface. The POC fluxes are generally highest in the western Arabian Sea during the SWM
40 (>20 $\text{mgC m}^{-2} \text{d}^{-1}$ equal to > 1.7 $\text{mmolC m}^{-2} \text{d}^{-1}$) where large seasonal variations in flux (7-24
41 $\text{mgC m}^{-2} \text{d}^{-1} = 0.6\text{-}2 \text{ mmolC m}^{-2} \text{d}^{-1}$) are also observed (Honjo et al., 1999; Rixen et al., 2019b).
42 In contrast, POC fluxes at 2000 meters are generally much lower in the central Arabian Sea (4-
43 12 $\text{mgC m}^{-2} \text{d}^{-1} = 0.25\text{-}0.5 \text{ mmolC m}^{-2} \text{d}^{-1}$) with the highest fluxes (> 10 $\text{mgC m}^{-2} \text{d}^{-1}$ equal to >
44 0.8 $\text{mmolC m}^{-2} \text{d}^{-1}$) also occurring during SWM, though with much less pronounced seasonal
45 variations (Rixen et al., 2019; Honjo et al., 1999). These patterns of POC flux in the Arabian
46 Sea are broadly consistent with organic carbon burial and sediment accumulation rates calculated

1 by Janke (1996), though with the latter an order of magnitude lower (Figure 9; <5 to >50 μmolC
2 $\text{m}^{-2} \text{yr}^{-1}$ which is equal to <0.01 to $>.14$ $\mu\text{molC} \text{m}^{-2} \text{d}^{-1}$). Major flux events are also observed in
3 the western Arabian Sea during both the SWM and NEM in association with passing eddies and
4 wind-curl events; these events can dominate the annual mass flux (Honjo et al., 1999). ²³⁴Th-
5 estimated POC export fluxes in the Arabian Sea reveal similar spatial and temporal patterns with
6 POC export efficiencies varying from <2 to 5% (Subha Anand et al, 2018a,b).

8 **3.4.2 Bay of Bengal**

9
10 Some of the highest concentrations of DOC in the Bay of Bengal (75 - 100 $\mu\text{molC/kg}$) are
11 observed in the near-surface (< 50 meters) waters of the northern Bay of Bengal, primarily due to
12 the large inputs of fresh water and terrigenous DOC from rivers (Hansell, 2009; Shah et al.,
13 2018; Figure 7). In addition, this fresh water enhances near-surface stratification which helps to
14 maintain the elevated DOC concentrations because it inhibits vertical mixing, as discussed
15 above. The concentration of DOC in the upper ocean in the Bay of Bengal also exhibits a
16 significant relationship with Chlorophyll-a, POC and DOC exudation rates, suggesting possible
17 sources through in situ biological processes (Rao and Sarma, 2022). Elevated DOC
18 concentrations are also observed to > 200 meters depth in the Bay of Bengal due to the
19 remineralization of sinking POM from the surface waters (Shah et al., 2018; Figure 7). Near-
20 surface DOC concentrations tend to decline at lower latitudes ($<14^\circ\text{N}$, Hansell, 2009; Shah et al.,
21 2018). Rao et al. (2021) report that about half of the primary production in the Bay of Bengal is
22 released as DOC during the summer monsoon due to existence of oligotrophic conditions, warm
23 waters and dominance of picophytoplankton biomass and Shah et al. (2018) estimate that DOC
24 remineralization fuels $\sim 18\%$ of the apparent oxygen utilization. As observed in the Arabian Sea,
25 DOC concentrations below 500 meters in the Bay of Bengal are low (<50 $\mu\text{molC/kg}$) and
26 relatively uniform across the basin, and there appears to be little impact of the OMZ on DOC
27 concentrations (Figure 7).

28
29 In the Bay of Bengal, the near-surface concentrations of POC can vary from < 4 to > 10 $\mu\text{mol/kg}$
30 depending on location and season (Fernandes et al., 2009; Figure 12). Spatial and temporal
31 variations are smaller compared to the Arabian Sea with POC concentrations varying from 4.3 to
32 11.1 $\mu\text{molC/kg}$, 3.1 to 10.9 $\mu\text{molC/kg}$, and 4.3 to 9.0 $\mu\text{molC/kg}$ during SWM, fall intermonsoon,
33 and spring intermonsoon, respectively, in one study (Fernandes et al. 2009). In contrast to the
34 Arabian Sea, POC and chlorophyll concentrations can be higher offshore compared to coastal
35 stations in the Bay of Bengal, especially during SWM (Fernandes et al., 2009; Vinayachandran,
36 2009; Thushara et al., 2019). These elevated offshore POC and chlorophyll concentrations are
37 not, however, revealed by remote sensing. Rather, the satellite estimates generally indicate that
38 the highest concentrations occur near the coast (Gardner et al., 2006; Figure 8). As in the
39 Arabian Sea, POC and chlorophyll concentrations are correlated in the Bay of Bengal with
40 subsurface chlorophyll maxima generally deeper and more pronounced, as discussed above (e.g.,
41 Fernandes et al., 2009). In general, POC concentrations and percent POC contribution to the
42 total suspended particulate matter tends to decrease with increasing water column depth
43 indicating heterotrophic remineralization of sinking particles (Fernandes et al., 2009). High
44 chlorophyll concentrations and high Chl a /POC ratios observed during the SWM and fall
45 intermonsoon indicate the presence of relatively fresh POM in the Bay Bengal during these two
46 seasons (Fernandes et al., 2009). POC concentration measured during the spring intermonsoon

1 were lowest in the southern Bay of Bengal (0.51–0.65 $\mu\text{molC/kg}$, Subha Anand et al., 2017). In
2 general, seasonal and spatial differences in river influence, combined with physical forces such
3 as eddies and mixing/entrainment that pump nutrients into the euphotic zone, drive seasonal and
4 spatial variations in the quantity and quality of POM in the Bay of Bengal (Fernandes et al.,
5 2009; Vinayachandran, 2009; Subha Anand et al., 2017; Thushara et al., 2019).

6
7 POC export normalized to 2000 meters in the Bay of Bengal is generally lower and less strongly
8 seasonal than in the Arabian Sea, with fluxes varying between 2 and 14 $\text{mgC m}^{-2} \text{d}^{-1}$ (= 0.17 –
9 1.2 $\text{mmolC m}^{-2} \text{d}^{-1}$; Rixen et al., 2019b). In contrast, POC export from the euphotic zone in the
10 Sri Lanka Dome region estimated from the satellite-derived net primary production data and
11 export fluxes calculated with a model give 118.5 and 427.4 $\text{mgC m}^{-2} \text{d}^{-1}$ (equal to 9.8 and 35.6
12 $\text{mmolC m}^{-2} \text{d}^{-1}$), respectively (Sreeush et al., 2018), again suggesting dramatic declines in export
13 at depth compared to the surface. In general, riverine freshwater and nutrient inputs to the Bay
14 of Bengal increase POC export near the coast. This pattern is revealed by ^{234}Th -estimated POC
15 export flux in the Bay of Bengal during the NEM, which varies from 0.1 to 1.6 $\text{mmolC m}^{-2} \text{d}^{-1}$
16 with the highest flux observed in the east Indian coastal zone (Subha Anand et al., 2017). These
17 patterns of POC flux are also broadly consistent with organic carbon burial and sediment
18 accumulation rates calculated by Janke (1996), where the former are highest along the east coast
19 of India (Figure 9). Though, as in the Arabian Sea, the organic carbon burial rates estimated by
20 Janke (1996) are an order of magnitude lower than the POC fluxes normalized to 2000 meters
21 from Rixen et al. (2019).

22 23 **3.4.3 Equatorial waters, Indonesian Throughflow, and the Leeuwin Current**

24
25 A modeling study reported by Hansell (2009) and Hansell et al. (2009) suggests a zonal decline
26 in near-surface (30 meter) DOC concentrations along the equator in the Indian Ocean with values
27 dropping from $\sim 75 \mu\text{molC/kg}$ in the east off of northern Sumatra to $< 70 \mu\text{molC/kg}$ in the west
28 off of central east Africa. This pattern appears to be linked to the aforementioned declines in
29 near-surface DOC concentrations to $< 70 \mu\text{molC/kg}$ that are associated with upwelling along the
30 western side of the basin (Hansell and Peltzer, 1998; Hansell, 2009). The modeling study
31 reported by Hansell (2009) and Hansell et al. (2009) also suggests that near-surface DOC
32 concentrations are elevated to $> 75 \mu\text{molC/kg}$ in an open ocean region between 10° and 20°S and
33 80° and 100°E coincident with shallow OMZ (Figure 1), minimum sedimentation rate (Figure 9),
34 and lower salinity (Figure 5), and that concentrations decline eastward to $< 70 \mu\text{molC/kg}$ in the
35 the Indonesian Throughflow region and in the Leeuwin Current, but these features are not readily
36 apparent in meridional or zonal sections (Figure 7). DOC concentrations below 500 meters in
37 these waters are also low ($< 50 \mu\text{molC/kg}$) and uniform (Figure 7).

38
39 Satellite-estimated near-surface POC concentrations in open ocean equatorial waters of the
40 Indian Ocean are generally low ($< 60 \text{mgC m}^{-3}$ which is equal to $< 5 \mu\text{molC/kg}$) with
41 concentrations increasing during the SWM, especially in the west due to the aforementioned
42 influence of coastal upwelling (Gardner et al., 2006; Figure 8). Elevated POC concentrations ($>$
43 72mgC/m^3 which is equal to $> 6 \mu\text{molC/kg}$) are also observed in the eastern equatorial Indian
44 Ocean along the coast off Sumatra and Java and in the Indonesian Throughflow region,
45 particularly during the SEM. All of these regions of elevated POC are associated with elevated
46 chlorophyll concentrations ($> 0.4\%$ of POC; Figure 8, Gardner et al., 2006). Unsurprisingly,

1 POC and chlorophyll concentrations are generally low along the coast of western Australia
2 where the downwelling Leeuwin Current flows southward (Figure 8). Estimated organic carbon
3 burial rates show similar patterns, i.e., low rates ($< 5 \text{ mmolC m}^{-2} \text{ yr}^{-1}$) in open ocean equatorial
4 waters and higher rates in the west and east in association with upwelling and the influence of
5 the Indonesian Throughflow (Janke, 1996; Figure 9). Surprisingly, estimated organic carbon
6 burial rates are distinctly elevated ($5\text{-}10 \text{ mmolC m}^{-2} \text{ yr}^{-1}$) along the coast of Western Australia
7 (Janke, 1996; Figure 9), likely due to coastal mixing processes, intermittent localized upwelling
8 and eddy generation in the otherwise oligotrophic downwelling Leeuwin Current (Hood et al.,
9 2017).

10
11 ^{234}Th -estimates of POC export flux have revealed elevated values in eastern-central equatorial
12 waters of the Indian Ocean during spring intermonsoon (up to $7.7 \text{ mmolC m}^{-2} \text{ d}^{-1}$) in association
13 with elevated rates of primary production (Subha Anand et al., 2017). These elevated rates are
14 somewhat surprising given the downwelling circulation that is associated with the eastward-
15 flowing equatorial currents (Strutton et al., 2015), but they are consistent with eastward increases
16 in organic carbon burial and sedimentation rates along the equator (Janke, 1996; Figure 9). They
17 are also consistent with eastward increases POC export from the euphotic zone estimated from
18 the satellite-derived net primary production data and export fluxes calculated with a model that
19 give 149.4 and $590.5 \text{ mgC m}^{-2} \text{ d}^{-1}$ (equal to 12.54 and $49.2 \text{ mmolC m}^{-2} \text{ d}^{-1}$), respectively, off
20 Sumatra, compared to similarly estimated values of 110.8 and $220.1 \text{ mgC m}^{-2} \text{ d}^{-1}$ (equal to 9.2
21 and $18.3 \text{ mmolC m}^{-2} \text{ d}^{-1}$), respectively, in the Seychelles-Chagos Thermocline Ridge region
22 (Sreeush et al., 2018).

23
24 There are few direct measurements of POC concentrations and export flux off of western
25 Australia. Waite et al. (2016) has shown that mesoscale eddies generated by the Leeuwin Current
26 can strongly impact carbon export fluxes. Specifically, the subsurface distribution of particles in
27 these eddies funnel into a wineglass shape down to 1000 m (Figure 13), leading to a sevenfold
28 increase of vertical carbon flux in the eddy center versus the eddy flanks. This is consistent with
29 the aforementioned idea that eddy generation in the Leeuwin Current gives rise to elevated
30 organic carbon burial rates along the coast of Western Australia (Janke, 1996; Figure 9).

31 32 **3.4.4 Southwestern Indian Ocean**

33
34 Although the modeling study reported by Hansell (2009) and Hansell et al. (2009) suggests that
35 near-surface (30 meter) DOC concentrations are lower ($< 65 \text{ }\mu\text{molC/kg}$) in the southwestern
36 Indian Ocean and in the Mozambique Channel, these declines are not apparent in zonal sections
37 (e.g., Figure 7). Rather, a meridional section along $\sim 30^\circ \text{ E}$ (IO6N from Arctica to western South
38 Africa) shows a very clear increase in near-surface ($< 50 \text{ meter}$) DOC concentrations north of
39 45° S from $< 50 \text{ }\mu\text{molC/kg}$ to $> 70 \text{ }\mu\text{molC/kg}$ (Hansel, 2009; Figure 7). Moreover, these elevated
40 concentrations extend downward to $> 300 \text{ meters}$ depth (Figure 7). These data suggest that the
41 Agulhas Current advects relatively high tropical and subtropical DOC concentrations
42 southwestward along the coast of South Africa and also eastward in the Agulhas Retroflexion,
43 and that these elevated concentrations are being mixed downward in the current. This
44 speculation is consistent with the fact that the Agulhas Current extends to $> 1000 \text{ meters}$ depth
45 and is derived from oligotrophic tropical and subtropical sources waters (Hood et al., 2017) that

1 have relatively high DOC concentrations (Figure 7). DOC concentrations below 1000 meters in
2 these waters are low ($<50 \mu\text{molC/kg}$) and relatively uniform (Figure 7).

3
4 Satellite estimates suggest that POC concentrations are generally low ($< 72 \text{ mgC m}^{-3}$ which is
5 equal to $< 6 \mu\text{molC/kg}$) in the southwestern Indian Ocean and in the Agulhas Current during both
6 the austral summer and winter seasons (Gardner et al., 2006; Figure 8). But some elevated POC
7 concentrations ($> 72 \text{ mgC/m}^3$, $> 6 \mu\text{molC/kg}$) are observed in the austral winter in the
8 Mozambique Channel, along the southwestern coast of South Africa, over the Agulhas Bank and
9 in the Agulhas retroflection (Gardner et al., 2006; Figure 8). All of these regions are associated
10 with elevated chlorophyll concentrations ($> .4\%$ of POC; Figure 8, Gardner et al., 2006). In the
11 Mozambique Channel the elevated concentrations are associated with entrainment and offshore
12 advection of coastal POM in eddies (Kolasinsky et al., 2012), whereas the elevated POM
13 concentrations along the southwestern coast of South Africa and over the Agulhas Bank are
14 associated with wind-induced and topographically controlled coastal upwelling (Hood et al.,
15 2017; Hood et al., 2021, this volume). The tongue of elevated POC and chlorophyll
16 concentration that is associated with the Agulhas retroflection is particularly striking (Figure 8).
17 This is a region where strong eastward flows and persistent eddies are observed (Pazan and
18 Niiler, 2004). It is possible that these eddies mix or upwell nutrients into the euphotic zone,
19 fueling a low level of primary production. This region of elevated POC and chlorophyll extends
20 all the way to the Kerguelen Islands during the austral summer (Figure 8; Gardner et al., 2006).

21
22 Estimated organic carbon burial rates in the southwestern Indian Ocean range from $< 5 - \sim 10$
23 $\text{mmolC m}^{-2} \text{ yr}^{-1}$ with the highest rates observed along the coastal zone of southeastern Africa
24 (Janke, 1996; Figure 9). Interestingly, these estimates also clearly show elevated organic carbon
25 burial (and sedimentation) rates in the same region where there is a tongue of elevated near-
26 surface POC and chlorophyll concentration associated with the Agulhas retroflection (Gardner et
27 al., 2006; compare Figures 8 and 9). These elevated carbon burial rates also extend all the way
28 to the Kerguelen Islands. This is in contrast to the low carbon burial rates ($< 5 \text{ mmolC m}^{-2} \text{ yr}^{-1}$;
29 Janke, 1996; Figure 9) and low ^{234}Th -estimated POC export fluxes (from 0.10 to 2.53 mmolC m^{-2}
30 d^{-1} below 100m) that are observed slightly further south (Coppola et al., 2005).

31 32 **3.4.5 Southern subtropical gyre**

33
34 Near surface (< 50 meters) DOC concentrations in the southern subtropical gyre of the Indian
35 Ocean are significantly elevated ($> 75 \mu\text{molC/kg}$) between 10° and 35° S (Figure 7), consistent
36 with the positive correlation between DOC concentrations and temperature, i.e., the southern
37 subtropical gyre is warm and stratified and DOC concentrations become elevated because there
38 is reduced vertical mixing. Near-surface DOC concentrations decline precipitously to < 50
39 $\mu\text{molC/kg}$ south of 40° S due to increased vertical mixing in the higher latitude waters (Figure
40 7). There is also evidence of subduction and northward transport of DOC in the subtropical
41 front between 10° and 35° S where elevated DOC concentrations can be seen extending to > 250
42 meters depth (Figure 7). The source of this subducted water has DOC concentrations between
43 65 and 70 $\mu\text{molC/kg}$, and as this water moves downward and equatorward the DOC is
44 remineralized, dropping to $\sim 55 \mu\text{molC/kg}$ at 250 meters depth (Hansell, 2009; Figure 7). DOC
45 concentrations below 500 meters in the southern subtropical Indian Ocean are also low (< 50
46 $\mu\text{molC/kg}$) and relatively uniform (Figure 7).

1
2 The lowest POC concentrations ($< 48 \text{ mgC/m}^3$ equal to $< 4 \text{ umolC/kg}$) in the Indian Ocean are
3 observed in the oligotrophic southern subtropical gyre. These low POC values are associated
4 with low chlorophyll concentrations ($< .3\%$ of POC; Figure 8, Gardner et al., 2006). These low
5 POC and low percent chlorophyll waters dramatically increase in area during the Southern
6 Hemisphere summer due to increases in summer stratification and lower nutrient availability
7 (Gardner et al., 2006; Figure 8). Nonetheless, subsurface chlorophyll maxima exist below these
8 oligotrophic regions (see Hood et al., 2022, this volume). It is likely that the subsurface
9 chlorophyll maxima are associated with somewhat shallower subsurface POC maxima, with the
10 latter weaker as discussed above.

11
12 Sediment trap-measured POC fluxes in the southern subtropical gyre of the Indian Ocean are
13 some of the lowest recorded worldwide ($\sim 0.50 \text{ mgC m}^{-2} \text{ day}^{-1} = 0.04 \text{ mmolC m}^{-2} \text{ d}^{-1}$, measured at
14 500–600 and 2600–3500 meters; Harms et al., 2021). Low POC fluxes are consistent with the
15 extremely low organic carbon burial ($< 2 \text{ mmolC m}^{-2} \text{ yr}^{-1}$) and sediment accumulation rates
16 calculated by Janke (1996; Figure 9). These low POC fluxes are the result of the strongly
17 stratified, nutrient-depleted and low productivity near-surface waters in the gyre (Harms et al.,
18 2021; Hood et al., 2022; this volume). These continuously oligotrophic conditions result in an
19 almost constant POC fluxes in space and time. The lack of seasonality in the POC fluxes can also
20 be attributed to intense organic matter degradation in the water column (Harms et al., 2021). The
21 small amount of variability that is observed is related to variations wind-induced physical mixing
22 events and the passage of eddies. Preliminary estimates indicate that the average POC export
23 efficiency is extremely low ($\sim 0.03\%$) in these waters (Harms et al., 2021).

24 25 **5. Summary and conclusions**

26
27 The thickest OMZ in the world is found in the northern Indian Ocean in the Arabian Sea where
28 intermediate water ($\sim 200\text{-}800 \text{ m}$) oxygen concentrations decline to nearly zero, with consequent
29 impacts on nitrogen cycling. These impacts include denitrification-driven reductions in deep
30 NO_3^- concentrations, appearance of NO_2^- maxima, generation of greenhouse gases (N_2O) and
31 globally-significant losses of fixed nitrogen from the ocean. In contrast, these biogeochemical
32 impacts are not observed in the Bay of Bengal where intermediate water dissolved oxygen
33 concentrations are poised just above the threshold below which denitrification becomes
34 significant. The low oxygen conditions in the water column in both the Arabian Sea and the Bay
35 of Bengal are associated with slow ventilation and high biological oxygen demand. It appears
36 that a weaker ballast effect and higher biological productivity sustain higher biological oxygen
37 consumption in the Arabian Sea compared to the Bay of Bengal, which balances the higher
38 physical oxygen supply in the Arabian Sea and explains its more intense OMZ.

39
40 The volume of hypoxic waters and denitrification in the Arabian Sea strongly increase in
41 response to increases in monsoon winds. Such increases in Arabian Sea denitrification are
42 expected to cause increases in N_2 and N_2O production. However, global syntheses of long term
43 OMZ variability reveal only a weak decrease of dissolved oxygen concentrations in the OMZs of
44 the Arabian Sea and the Bay of Bengal in comparison to OMZs of the South Atlantic Ocean and
45 the Pacific Ocean. Moreover, outbreaks of hydrogen sulfide have so far not been reported in the
46 northern Indian Ocean during the last 50 years, other than in bottom waters on the Indian shelf.

1 The absence of H₂S implies that the interplay between physical oxygen supply and the biological
2 oxygen consumption has largely maintained the current hypoxic/anoxic conditions in the
3 Arabian Sea and the Bay of Bengal OMZs. However, recent observational and modeling studies
4 indicate that oxygen concentrations are now decreasing in the Arabian Sea and that these
5 decreases are having significant biogeochemical and ecological impacts. Future evolution of the
6 northern Indian Ocean OMZs projected by Earth System models is highly uncertain.

7
8 The Indian Ocean remains one of the most poorly sampled ocean regions with respect to
9 inorganic and organic carbon pools and air-sea carbon fluxes. The system accounts for ~20% of
10 the global oceanic uptake of atmospheric CO₂. The Arabian Sea is a source of CO₂ to the
11 atmosphere due to elevated pCO₂ within the SWM-driven upwelling whereas it is still uncertain
12 whether the Bay of Bengal is a CO₂ source or sink due to the sparse spatial and temporal
13 sampling. South of 14°S the Indian Ocean appears to be a strong net CO₂ sink due to the
14 combined effects of both the solubility pump and the biological pump. Surface pH values in the
15 Indian Ocean are among the lowest of the major ocean basins, and the reasons for this are poorly
16 understood. Increases in sulphate and nitrogen aerosol loadings over the Bay of Bengal may be
17 mainly responsible for the increased acidity in the northwestern Bay of Bengal in recent years
18 and reduced river discharge together with a positive IOD event have also been shown to
19 contribute to enhanced acidification and pCO₂ levels in the coastal waters in the western Bay of
20 Bengal. Projected increases in oceanic CO₂ concentrations will lead to further acidification of the
21 Indian Ocean over the coming decades, with potentially severe negative impacts on coral reefs
22 and other calcifying organisms.

23
24 DOC concentrations in the Indian Ocean vary between ~40 and 80 μmolC/kg. DOC
25 concentrations in the Indian Ocean tend to be high in stratified near-surface tropical and
26 subtropical waters where DOC is produced and accumulates, and DOC concentrations are lowest
27 in the deep ocean where heterotrophic consumption of DOC exceeds autotrophic production. As
28 observed elsewhere in the global ocean, satellite-estimated near-surface POC concentrations are
29 elevated in coastal regions of the Indian Ocean with values often exceeding 120 mgC/m³ (= 10
30 μmolC/kg). The highest POC concentrations in the Indian Ocean are observed in the
31 northwestern part of the basin in the Arabian Sea and off the coast of Somalia with values
32 estimated to be greater than 96 mgC/m³ (= 8 μmolC/kg). These high POC values are associated
33 with high chlorophyll concentrations. The lowest POC concentrations (< 48 mgC/m³ = 4
34 μmolC/kg) are observed in the oligotrophic southern subtropical gyre. These low POC values
35 are associated with low chlorophyll concentrations.

36
37 The spatial and temporal variability in POC export flux in the Indian Ocean is similar to the
38 above mentioned patterns in POC and chlorophyll concentration, consistent with primary
39 production as the main control on the spatial and temporal variability of organic carbon fluxes.
40 However, in river-influence regions, like the Bay of Bengal, the spatial variability of organic
41 carbon flux is also strongly influenced by lithogenic matter content. In the Arabian Sea POC
42 export at 2000 meters ranges from < 6 to > 22 mgC m⁻² d⁻¹ (< 0.5 to > 1.8 mmolC m⁻² d⁻¹) with
43 the highest fluxes observed during the SWM. In contrast, POC export at 2000 meters in the Bay
44 of Bengal is generally lower and less strongly seasonal than in the Arabian Sea with fluxes
45 varying between 2 and 14 mgC m⁻² d⁻¹ (0.17 to 1.1 mmolC m⁻² d⁻¹). ²³⁴Th-estimates of POC
46 export flux have revealed elevated values in eastern-central equatorial waters of the Indian

1 Ocean (up to $7.7 \text{ mmolC m}^{-2} \text{ d}^{-1}$) in association with elevated rates of primary production. These
2 elevated rates are surprising given the downwelling equatorial circulation, but they are consistent
3 with zonal variations in satellite and model-based estimates of near surface POC export flux and
4 organic carbon burial rates. There are few direct measurements of POC concentrations and
5 export flux off of Western Australia where estimated organic carbon burial rates are distinctly
6 elevated, perhaps due to the influence of Leeuwin Current eddies. Estimated organic carbon
7 burial rates in the southwestern Indian Ocean range from $< 5 - \sim 10 \text{ mmolC m}^{-2} \text{ yr}^{-1}$, with the
8 highest rates observed along the coastal zone of southeastern Africa and in the Agulhas
9 retroflection. POC export fluxes in the southern subtropical gyre of the Indian Ocean are some
10 of the lowest recorded worldwide ($\sim 0.50 \text{ mgC m}^{-2} \text{ d}^{-1} = 0.04 \text{ mmolC m}^{-2} \text{ d}^{-1}$).

11
12 As in the other ocean basins, it is clear that there is a strong connection in the Indian Ocean
13 between the physics that drives (or suppresses) nutrient delivery to the photic zone and responses
14 of oxygen, CO_2 flux, pH, DOC, POC and POC export. Monsoonal wind forcing is a major driver
15 of biogeochemical variability throughout the northern Indian Ocean and in equatorial waters. In
16 addition, there are regionally specific processes that significantly modulate oxygen, CO_2 flux,
17 pH, DOC, POC and POC export. For example, upwelling and strong advective impacts in the
18 Arabian Sea; freshwater and stratification in the Bay of Bengal; the influence of ITF, poleward
19 transport, downwelling and eddies in the southeastern Indian Ocean; and poleward transport of
20 tropical waters, combined with localized upwelling in the southwestern Indian Ocean. The
21 southern subtropical gyre is extremely oligotrophic.

22
23 Observational and modeling research should be aimed at improving understanding of northern
24 Indian Ocean OMZ variability at seasonal and decadal time scales. Further, uncertainty in future
25 projections needs to be reduced. Additional observations are also needed to better constrain air-
26 sea CO_2 fluxes and the carbon cycle in general. Measurements of CO_2 and DOC concentrations,
27 capturing spatial and temporal variability, are particularly sparse. This improved understanding
28 is needed to predict the impacts of anthropogenic influence and global warming on Indian Ocean
29 biogeochemistry and ecosystems and also for understanding the role of the Indian Ocean in
30 global ocean biogeochemical cycles both now and in the future.

31 32 **6. Educational Resources**

33
34 -Ocean Data View, free software for plotting oceanographic data. Available at:

35 <https://odv.awi.de>

36
37 -World Ocean Atlas, a collection of objectively analyzed, quality controlled temperature,
38 salinity, oxygen, phosphate, silicate, and nitrate means based on profile data from the World
39 Ocean Database. Available at: <https://www.ncei.noaa.gov/products/world-ocean-atlas>

40
41 -Surface Ocean CO_2 Atlas (SOCAT) is a synthesis of quality-controlled, surface ocean $f\text{CO}_2$
42 (fugacity of carbon dioxide) observations by the international marine carbon research
43 community. Available at: <https://www.socat.info>

44
45 -Satellite ocean color data. Available at: <https://oceancolor.gsfc.nasa.gov>

46

1 **Acknowledgements**

2
3 The development of this article was supported by the Scientific Committee for Oceanic Research
4 (SCOR) via direct funding to the Second International Indian Ocean Expedition (IIOE-2) and
5 indirect funding through the Integrated Marine Biosphere Research (IMBeR) regional program
6 SIBER (Sustained Indian Ocean Biogeochemistry and Ecosystem Research). Additional support
7 was provided by NASA grant no. 80NSSC17K0258 49A37A, NOAA grant no.
8 NA15NMF4570252 NCRS-17, and NSF grant no. 2009248 to R. Hood. The Ocean Data View
9 software package (<https://odv.awi.de>) was used in developing this article's original graphics. The
10 article also benefitted from extensive comments provided by Dr. V.V.S.S. Sarma and one
11 anonymous reviewer. This is UMCES contribution YYYY.

13 **Author contributions**

14
15 All authors contributed to writing of the text, discussion of content, and structure
16 of the chapter.

18 **Index Terms**

19
20 Indian Ocean, Arabian Sea, Bay of Bengal, Indonesian Throughflow, Leeuwin
21 Current, Mozambique Channel, Agulhas Current, Indian Ocean southern
22 subtropical gyre, oxygen, oxygen minimum zone, salinity, stratification,
23 denitrification, N₂O, CO₂, pH, dissolved organic carbon (DOC), particulate organic
24 carbon (POC), carbon export flux.

26 **References**

- 27
28 Acharya, Shiba Shankar, and Mruganka K Panigrahi. 2016. 'Eastward shift and maintenance of
29 Arabian Sea oxygen minimum zone: Understanding the paradox', *Deep Sea Research*
30 *Part I: Oceanographic Research Papers*, 115: 240-52.
- 31 Al Azhar, Muchamad, Zouhair Lachkar, Marina Lévy, and Shafer Smith. 2017. 'Oxygen
32 minimum zone contrasts between the Arabian Sea and the Bay of Bengal implied by
33 differences in remineralization depth', *Geophysical Research Letters*, 44: 11,106-11,14.
- 34 Altabet, M. A., R. Francois, D. W. Murray, and W. L. Prell. 1995. 'Climate-related variations in
35 denitrification in the Arabian Sea from sediment N-15/N-14 ratios', *Nature*, 373: 506-09.
- 36 Altabet, Mark A, Matthew J Higginson, and David W Murray. 2002. 'The effect of millennial-
37 scale changes in Arabian Sea denitrification on atmospheric CO₂', *Nature*, 415: 159-62.
- 38 Altieri, Andrew H, Seamus B Harrison, Janina Seemann, Rachel Collin, Robert J Diaz, and
39 Nancy Knowlton. 2017. 'Tropical dead zones and mass mortalities on coral reefs',
40 *Proceedings of the National Academy of Sciences*, 114: 3660-65.

- 1 Anand, S Subha, R Rengarajan, Damodar Shenoy, Mangesh Gauns, and SWA Naqvi. 2018.
2 'POC export fluxes in the Arabian Sea and the Bay of Bengal: A simultaneous
3 $^{234}\text{Th}/^{238}\text{U}$ and $^{210}\text{Po}/^{210}\text{Pb}$ study', *Marine Chemistry*, 198: 70-87.
- 4 Anju, M, V Valsala, BR Smitha, G Bharathi, and CV Naidu. 2022. 'Observed denitrification in
5 the northeast Arabian Sea during the winter-spring transition of 2009', *Journal of Marine*
6 *Systems*, 227: 103680.
- 7 Antoine, David, Jean-Michel André, and André Morel. 1996. 'Oceanic primary production: 2.
8 Estimation at global scale from satellite (coastal zone color scanner) chlorophyll', *Global*
9 *Biogeochemical Cycles*, 10: 57-69.
- 10 Bahl, A, A Gnanadesikan, and M-A Pradal. 2019. 'Variations in ocean deoxygenation across
11 earth system models: Isolating the role of parameterized lateral mixing', *Global*
12 *Biogeochemical Cycles*, 33: 703-24.
- 13 Bakker, D. C. E., and et al. 2014. 'An update to the Surface Ocean CO₂ Atlas (SOCAT version
14 2)', *Earth Systems Science Data*, 6: 69-90.
- 15 Bange, H. W., and et. al. 2000. 'A revised nitrogen budget for the Arabian Sea', *Global*
16 *Biogeochemical Cycles*, 14: 1283-97.
- 17 Bange, Hermann W, MO Andreae, S Lal, CS Law, SWA Naqvi, PK Patra, T Rixen, and RC
18 Upstill-Goddard. 2001. 'Nitrous oxide emissions from the Arabian Sea: A synthesis',
19 *Atmospheric Chemistry and Physics*, 1: 61-71.
- 20 Banse, K, SWA Naqvi, PV Narvekar, JR Postel, and DA Jayakumar. 2014. 'Oxygen minimum
21 zone of the open Arabian Sea: variability of oxygen and nitrite from daily to decadal
22 timescales', *Biogeosciences*, 11: 2237-61.
- 23 Bates, N. R., A. C. Pequignet, and C. L. Sabine. 2006. 'Ocean carbon cycling in the Indian
24 Ocean: I. Spatio-temporal variability of inorganic carbon and air-sea CO₂ gas exchange',
25 *Global Biogeochemical Cycles*, 20: GB3020.
- 26 Bednarsek, N., G. A. Tarling, D. C. E. Bakker, S. Fielding, E. M. Jones, H. J. Venables, P. Ward,
27 A. Kuzirian, B. Leze, R. A. Feely, and E. J. Murphy. 2012. 'Extensive dissolution of live
28 pteropods in the Southern Ocean', *Nature Geoscience*, 5: 881-85.
- 29 Behrman, D. 1981. *Assault on the Largest Unknown: the International Indian Ocean Expedition,*
30 *1959-1965* (UNESCO Press: Paris).
- 31 Bercovici, SK, AP McNichol, L Xu, and DA Hansell. 2018. 'Radiocarbon content of dissolved
32 organic carbon in the South Indian Ocean', *Geophysical Research Letters*, 45: 872-79.
- 33 Bopp, L, Laure Resplandy, A Untersee, P Le Mezo, and M Kageyama. 2017. 'Ocean (de)
34 oxygenation from the Last Glacial Maximum to the twenty-first century: insights from
35 Earth System models', *Philosophical Transactions of the Royal Society A: Mathematical,*
36 *Physical and Engineering Sciences*, 375: 20160323.
- 37 Bopp, Laurent, Laure Resplandy, James C Orr, Scott C Doney, John P Dunne, M Gehlen, P
38 Halloran, Christoph Heinze, Tatiana Ilyina, and Roland Seferian. 2013. 'Multiple

- 1 stressors of ocean ecosystems in the 21st century: projections with CMIP5 models',
2 *Biogeosciences*, 10: 6225-45.
- 3 Boyd, Philip W, Hervé Claustre, Marina Levy, David A Siegel, and Thomas Weber. 2019.
4 'Multi-faceted particle pumps drive carbon sequestration in the ocean', *Nature*, 568: 327-
5 35.
- 6 Bristow, Laura A, Cameron M Callbeck, Morten Larsen, Mark A Altabet, Julien
7 Dekaezemacker, Michael Forth, M Gauns, Ronnie N Glud, Marcel MM Kuypers, and
8 Gaute Lavik. 2017. 'N₂ production rates limited by nitrite availability in the Bay of
9 Bengal oxygen minimum zone', *Nature Geoscience*, 10: 24-29.
- 10 Cabré, Anna, Irina Marinov, Raffaele Bernardello, and Daniele Bianchi. 2015. 'Oxygen
11 minimum zones in the tropical Pacific across CMIP5 models: mean state differences and
12 climate change trends', *Biogeosciences*, 12: 5429-54.
- 13 Canfield, Don E, Beate Kraft, Carolin R Löscher, Richard A Boyle, Bo Thamdrup, and Frank J
14 Stewart. 2019. 'The regulation of oxygen to low concentrations in marine oxygen-
15 minimum zones', *Journal of Marine Research*, 77: 297-324.
- 16 Carruthers, JN, SS Gogate, JR Naidu, and T Laevastu. 1959. 'Shorewards upslope of the layer of
17 minimum oxygen off Bombay: Its influence on marine biology, especially fisheries',
18 *Nature*, 183: 1084-87.
- 19 Cerutti, Julia, April J Burt, Philip Haupt, Nancy Bunbury, Peter J Mumby, and Gabriela
20 Schaeppman-Strub. 2020. 'Impacts of the 2014–2017 global bleaching event on a protected
21 remote atoll in the Western Indian Ocean', *Coral Reefs*, 39: 15-26.
- 22 Chakraborty, Kunal, Vinu Valsala, Trishneeta Bhattacharya, and Jayashree Ghosh. 2021.
23 'Seasonal cycle of surface ocean pCO₂ and pH in the northern Indian Ocean and their
24 controlling factors', *Progress in Oceanography*, 198: 102683.
- 25 Chakraborty, Kunal, Vinu Valsala, GVM Gupta, and VVSS Sarma. 2018. 'Dominant biological
26 control over upwelling on pCO₂ in sea east of Sri Lanka', *Journal of Geophysical
27 Research: Biogeosciences*, 123: 3250-61.
- 28 Codispoti, L., J. A. Brandes, J. Christensen, A. Devol, S. Naqvi, H. W. Paerl, and T. Yoshinari.
29 2001. 'The oceanic fixed nitrogen and nitrous oxide budgets: Moving targets as we enter
30 the anthropocene?', *Scientia Marina (Barcelona)*, 65, suppl. 2: 85-105.
- 31 Coppola, L, M Roy-Barman, S Mulsow, P Povinec, and C Jeandel. 2005. 'Low particulate
32 organic carbon export in the frontal zone of the Southern Ocean (Indian sector) revealed
33 by 234Th', *Deep Sea Research Part I: Oceanographic Research Papers*, 52: 51-68.
- 34 Cullen, John J. 2015. 'Subsurface chlorophyll maximum layers: enduring enigma or mystery
35 solved?', *Annual Review of Marine Science*, 7: 207-39.
- 36 Dalsgaard, T., D. E. Canfield, J. Petersen, B. Thamdrup, and J. Acuna-Gonzalez. 2003. 'N₂
37 production by the anammox reaction in the anoxic water column of Golfo Dulce, Costa
38 Rica', *Nature*, 422: 606-08.
- 39 de la Rocha, Christina, and Uta Passow. 2014. "The biological pump." In.: Elsevier Science.

- 1 de Moel, H., G. M. Ganssen, F. J. C. Peeters, S. J. A. Jung, D. Kroon, G. J. A. Brummer, and R.
2 E. Zeebe. 2009. 'Planktonic foraminiferal shell thinning in the Arabian Sea due to
3 anthropogenic ocean acidification?', *Biogeosciences*, 6: 1917-25.
- 4 de Verneil, Alain, Zouhair Lachkar, Shafer Smith, and Marina Lévy. 2021. 'Evaluating the
5 Arabian Sea as a regional source of atmospheric CO₂: seasonal variability and drivers',
6 *Biogeosciences Discussions*: 1-38.
- 7 Deutsch, C., J. L. Sarmiento, D. M. Sigman, N. Gruber, and J. P. Dunne. 2007. 'Spatial coupling
8 of nitrogen inputs and losses in the ocean', *Nature*, 445: 163-67.
- 9 DeVries, T, C Deutsch, PA Rafter, and F Primeau. 2013. 'Marine denitrification rates determined
10 from a global 3-D inverse model', *Biogeosciences*, 10: 2481-96.
- 11 Diaz, RJ, R Rosenberg, and K Sturdivant. 2019. 'Hypoxia in estuaries and semi-enclosed seas',
12 *Ocean deoxygenation: Everyone's problem*, edited by: Laffoley, D. and Baxter, JM,
13 IUCN, Gland, Switzerland.
- 14 Diaz, Robert J., and Rutger Rosenberg. 2008. 'Spreading Dead Zones and Consequences for
15 Marine Ecosystems', *Science*, 321: 926-29.
- 16 Dietrich, GÜNTER. 1936. 'Aufbau und Bewegung von Golfstrom und Agulhasstrom, eine
17 vergleichende Betrachtung', *Naturwissenschaften*, 24: 225-30.
- 18 Doney, S. C. 2010. 'The growing human footprint on coastal and open-ocean biogeochemistry',
19 *Science*, 328: 1512-16.
- 20 Dueser, WG, EH Ross, and ZJ Mlodzinska. 1978. 'Evidence for and rate of denitrification in the
21 Arabian Sea', *Deep Sea Research*, 25: 431-45.
- 22 Duteil, Olaf, and Andreas Oschlies. 2011. 'Sensitivity of simulated extent and future evolution of
23 marine suboxia to mixing intensity', *Geophysical Research Letters*, 38.
- 24 Eugster, Olivier, and Nicolas Gruber. 2012. 'A probabilistic estimate of global marine N-fixation
25 and denitrification', *Global Biogeochemical Cycles*, 26.
- 26 Fasham, Michael JR. 2003. 'JGOFS: a retrospective view.' in, *Ocean Biogeochemistry*
27 (Springer).
- 28 Feely, R. A., S. C. Doney, and S. R. Cooley. 2009. 'Ocean acidification: Present conditions and
29 future changes in a high-CO₂ world', *Oceanography*, 22: 36-47.
- 30 Feely, Richard A, Rik Wanninkhof, Simone Alin, John L Bullister, Gregory C Johnson, Jeremy
31 Mathis, Calvin W Mordy, Molly Baringer, and Jia-Zhong Zhang. 2005. 'Global Repeat
32 Hydrographic/CO₂/Tracer Surveys in Support of CLIVAR and Global Cycle Objectives:
33 Carbon Inventories and Fluxes'.
- 34 Fennel, Katja, and Emmanuel Boss. 2003. 'Subsurface maxima of phytoplankton and
35 chlorophyll: Steady-state solutions from a simple model', *Limnology and Oceanography*,
36 48: 1521-34.

- 1 Fernandes, Loreta, Narayan B Bhosle, SG Prabhu Matondkar, and Ravi Bhushan. 2009.
2 'Seasonal and spatial distribution of particulate organic matter in the Bay of Bengal',
3 *Journal of Marine Systems*, 77: 137-47.
- 4 Fine, Rana A. 1993. 'Circulation of Antarctic intermediate water in the South Indian Ocean',
5 *Deep Sea Research Part I: Oceanographic Research Papers*, 40: 2021-42.
- 6 Fuhrman, Jed A, and Douglas G Capone. 1991. 'Possible biogeochemical consequences of ocean
7 fertilization', *Limnology and Oceanography*, 36: 1951-59.
- 8 Garcia, H. E., R. A. Locarnini, T. P. Boyer, J. I. Antonov, M. M. Zweng, O. K. Baranova, and D.
9 R. Johnson. 2010. 'World Ocean Atlas 2009', *S. Levitus (Ed.), NOAA Atlas NESDIS 71,*
10 *Vol. 4, Washington, D. C., U.S. Government Printing Office.*
- 11 Gardner, WD, AV Mishonov, and MJ Richardson. 2006. 'Global POC concentrations from in-
12 situ and satellite data', *Deep Sea Research Part II: Topical Studies in Oceanography*, 53:
13 718-40.
- 14 Gattuso, J.-P., and L. Hansson. 2011. *Ocean Acidification* (Oxford University Press: Oxford,
15 UK).
- 16 Gaye, Birgit, Anna Böll, Joachim Segschneider, Nicole Burdanowitz, Kay-Christian Emeis,
17 Venkitasubramani Ramaswamy, Niko Lahajnar, Andreas Lückge, and Tim Rixen. 2018.
18 'Glacial–interglacial changes and Holocene variations in Arabian Sea denitrification',
19 *Biogeosciences*, 15: 507-27.
- 20 Gaye, Birgit, Birgit Nagel, Kirstin Dähnke, Tim Rixen, and Kay-Christian Emeis. 2013.
21 'Evidence of parallel denitrification and nitrite oxidation in the ODZ of the Arabian Sea
22 from paired stable isotopes of nitrate and nitrite', *Global Biogeochemical Cycles*, 27:
23 1059-71.
- 24 Gilson, Hugh Cary. 1933. 'The nitrogen cycle', *The John Murray Expedition*, 1934: 21-81.
- 25 Gnanadesikan, A, JP Dunne, and J John. 2012. 'Understanding why the volume of suboxic
26 waters does not increase over centuries of global warming in an Earth System Model',
27 *Biogeosciences*, 9: 1159-72.
- 28 Goes, Joaquim I, and Helga do R Gomes. 2016. 'An ecosystem in transition: the emergence of
29 mixotrophy in the Arabian Sea.' in, *Aquatic Microbial Ecology and Biogeochemistry: A*
30 *Dual Perspective* (Springer).
- 31 Goes, Joaquim I, Hongzhen Tian, Helga do Rosario Gomes, O Roger Anderson, Khalid Al-
32 Hashmi, Sergio deRada, Hao Luo, Lubna Al-Kharusi, Adnan Al-Azri, and Douglas G
33 Martinson. 2020. 'ecosystem state change in the Arabian Sea fuelled by the recent loss of
34 snow over the Himalayan-tibetan plateau region', *Scientific Reports*, 10: 1-8.
- 35 Gomes, H. D., J. I. Goes, S. G. P. Motondkar, E. J. Buskey, S. Basu, S. Parab, and P. G. Thoppil.
36 2014. 'Massive outbreaks of *Notiluca scintillans* blooms in teh Arabian Sea due to spread
37 of hypoxia', *Nature Communications*, 5: <http://dx.doi.org/10.1038/ncomms5862>.
- 38 Gould, John, Bernadette Sloyan, and Martin Visbeck. 2013. 'In situ ocean observations: A brief
39 history, present status, and future directions.' in, *International Geophysics* (Elsevier).

- 1 Graham, N. A. J., S. K. Wilson, S. Jennings, N. V. C. Polunin, J. Robinson, J. P. Bijoux, and T.
2 M. Daw. 2007. 'Lag effects in the impacts of mass coral bleaching on coral reef fish,
3 fisheries, and ecosystems', *Conservation Biology*, 21: 1291-300.
- 4 Gruber, N., and J. L. Sarmiento. 1997. 'Global patterns of marine nitrogen fixation and
5 denitrification', *Global Biogeochemical Cycles*, 11: 235-66.
- 6 Gruber, Nicolas. 2004. 'The dynamics of the marine nitrogen cycle and its influence on
7 atmospheric CO₂ variations.' in, *The ocean carbon cycle and climate* (Springer).
- 8 Gruber, Nicolas, and James N Galloway. 2008. 'An Earth-system perspective of the global
9 nitrogen cycle', *Nature*, 451: 293-96.
- 10 Gundersen, J. S., W. D. Gardner, M. J. Richardson, and I. D. Walsh. 1998. 'Effects of
11 monsoons on the seasonal and spatial distributions of POC and chlorophyll in the
12 Arabian Sea', *Deep Sea Research Part II*, 45: 2103-32.
- 13 Gupta, GVM, R Jyothibabu, Ch V Ramu, A Yudhistir Reddy, KK Balachandran, V Sudheesh,
14 Sanjeev Kumar, NVHK Chari, Kausar F Bepari, and Prachi H Marathe. 2021. 'The
15 world's largest coastal deoxygenation zone is not anthropogenically driven',
16 *Environmental Research Letters*, 16: 054009.
- 17 Gupta, GVM, V Sudheesh, KV Sudharma, N Saravanane, V Dhanya, KR Dhanya, G Lakshmi,
18 M Sudhakar, and SWA Naqvi. 2016. 'Evolution to decay of upwelling and associated
19 biogeochemistry over the southeastern Arabian Sea shelf', *Journal of Geophysical
20 Research: Biogeosciences*, 121: 159-75.
- 21 Gupta, R Sen, and SWA Naqvi. 1984. 'Chemical oceanography of the Indian Ocean, north of the
22 equator', *Deep Sea Research Part A. Oceanographic Research Papers*, 31: 671-706.
- 23 Haake, B, and V Ittekkot. 1990. 'Die Wind-getriebene „biologische Pumpe" und der
24 Kohlenstoffenzug im Ozean', *Naturwissenschaften*, 77: 75-79.
- 25 Hansell, Dennis A. 2009. 'Dissolved organic carbon in the carbon cycle of the Indian Ocean',
26 *Indian Ocean Biogeochemical Processes and Ecological Variability, Geophys. Monogr.
27 Ser*, 185: 217-30.
- 28 Hansell, Dennis A, Craig A Carlson, Daniel J Repeta, and Reiner Schlitzer. 2009. 'Dissolved
29 organic matter in the ocean: A controversy stimulates new insights', *Oceanography*, 22:
30 202-11.
- 31 Hansell, Dennis A, and Mónica V Orellana. 2021. 'Dissolved Organic Matter in the Global
32 Ocean: A Primer', *Gels*, 7: 128.
- 33 Hansell, Dennis A, and Edward T Peltzer. 1998. 'Spatial and temporal variations of total organic
34 carbon in the Arabian Sea', *Deep Sea Research Part II: Topical Studies in
35 Oceanography*, 45: 2171-93.
- 36 Harms, Natalie C, Niko Lahajnar, Birgit Gaye, Tim Rixen, Ulrich Schwarz-Schampera, and Kay-
37 Christian Emeis. 2021. 'Sediment trap-derived particulate matter fluxes in the
38 oligotrophic subtropical gyre of the South Indian Ocean', *Deep Sea Research Part II:
39 Topical Studies in Oceanography*: 104924.

- 1 Helly, J. J., and L. A. Levin. 2004. 'Global distribution of naturally occurring marine hypoxia on
2 continental margins', *Deep Sea Research Part I* 51: 1159-68.
- 3 Hoegh-Guldberg, O., and et. al. 2014. 'Chapter 30: The Ocean.' in IPCC WGII AR5 (ed.),
4 *Climate Change 2014: Impacts, Adaptation, and Vulnerability. Contribution of Working*
5 *Group II to the Fifth Assessment Report of the Intergovernmental Panel on Climate*
6 *Change* (Cambridge University Press: Cambridge, UK, and New York, NY, USA).
- 7 Hoegh-Guldberg, O., P. J. Mumby, A. J. Hooten, R. S. Steneck, P. Greenfield, E. Gomez, C. D.
8 Harvell, P. F. Sale, A. J. Edwards, K. Caldeira, N. Knowlton, C. M. Eakin, R. Iglesias-
9 Prieto, N. Muthiga, R. H. Bradbury, A. Dubi, and M. E. Hatziolos. 2007. 'Coral reefs
10 under rapid climate change and ocean acidification', *Science*, 318: 1737-42.
- 11 Honjo, S., J. Dymond, W. Prell, and V. Ittekkot. 1999. 'Monsoon-controlled export fluxes to the
12 interior of the Arabian Sea', *Deep-Sea Research (Part II, Topical Studies in*
13 *Oceanography)*, 46: 1859-902.
- 14 Hood, R. R. , H. W. Bange, L. Beal, L. E. Beckley, P. Burkill, G. L. Cowie, N. D'Adamo, G.
15 Ganssen, H. Hendon, J. Hermes, M. Honda, M. McPhaden, M. Roberts, S. Singh, E.
16 Urban, and W. Yu. 2015. "Science Plan of the Second International Indian Ocean
17 Expedition (IIOE-2): A Basin-Wide Research Program." In. Newark, Delaware, USA:
18 Scientific Committee on Oceanic Research.
- 19 Hood, R. R., L. E. B. Beckley, and J. D. Wiggert. 2017. 'Biogeochemical and ecological impacts
20 of boundary currents in the Indian Ocean', *Progress in Oceanography*, 156: 290-325.
- 21 Hood, R. R., V. J. Coles, J. Huggett, M. Landry, M. Levy, and J. W. Moffett. 2021. 'Nutrient,
22 phytoplankton and zooplankton variability in the Indian Ocean', *In: The Indian Ocean*
23 *and its role in the global climate system*, C. C. Ummenhofer and R. R. Hood (eds.),
24 *Elsevier*.
- 25 Howell, E. A., S. C. Doney, R. A. Fine, and D. B. Olson. 1997. 'Geochemical estimates of
26 denitrification in the Arabian Sea and the Bay of Bengal during WOCE', *Geophysical*
27 *Research Letters*, 24: 2549-52.
- 28 Hutchins, D. A., F.-X. Fu, Y. Zhang, M. E. Warner, Y. Feng, K. Portune, P. W. Bernhardt,
29 and M. R. Mulholland. 2007. 'CO₂ control of Trichodesmium N₂ fixation, photosynthesis,
30 growth rates, and elemental ratios: Implications for past, present, and future ocean
31 biogeography', *Limnology and Oceanography*, 52: 1293-304.
- 32 IPCC. 2007. 'Contribution of Working Groups I, II and III to the Fourth Assessment Report of
33 the Intergovernmental Panel on Climate Change.' in Core_Writing_Team, R. K. Pachauri
34 and A. Reisinger (eds.) (IPCC: Geneva, Switzerland).
- 35 ———. 2019. 'IPCC Special Report on the Ocean and Cryosphere in a Changing Climate'.
- 36 Ito, Takamitsu, Shoshiro Minobe, Matthew C Long, and Curtis Deutsch. 2017. 'Upper ocean O₂
37 trends: 1958–2015', *Geophysical Research Letters*, 44: 4214-23.
- 38 Ittekkot, V, RR Nair, S Honjo, Vo Ramaswamy, M Bartsch, S Manganini, and BN Desai. 1991.
39 'Enhanced particle fluxes in Bay of Bengal induced by injection of fresh water', *Nature*,
40 351: 385-87.

- 1 Ivanenkov, VN, and AG Rozanov. 1966. *Hydrogen sulphide contamination of the intermediate*
2 *layers of the Arabian Sea and the Bay of Bengal* (National Institute of Oceanography).
- 3 Jahnke, Richard A. 1996. 'The global ocean flux of particulate organic carbon: Areal distribution
4 and magnitude', *Global Biogeochemical Cycles*, 10: 71-88.
- 5 Kolasinski, Joanna, Sven Kaehler, and Sébastien Jaquemet. 2012. 'Distribution and sources of
6 particulate organic matter in a mesoscale eddy dipole in the Mozambique Channel (south-
7 western Indian Ocean): Insight from C and N stable isotopes', *Journal of Marine Systems*,
8 96: 122-31.
- 9 Kumar, M Dileep, SWA Naqvi, MD George, and DA Jayakumar. 1996. 'A sink for atmospheric
10 carbon dioxide in the northeast Indian Ocean', *Journal of Geophysical Research: Oceans*,
11 101: 18121-25.
- 12 Kuypers, M. M. M., A. O. Sliemers, G. Lavik, M. Schmid, B. B. Joergensen, J. G. Kuenen, J. S.
13 S. Damste, M. Strous, and M. S. M. Jetten. 2003. 'Anaerobic ammonium oxidation by
14 anammox bacteria in the Black Sea', *Nature*, 422: 608-11.
- 15 Kwiatkowski, Lester, Olivier Torres, Laurent Bopp, Olivier Aumont, Matthew Chamberlain,
16 James R Christian, John P Dunne, Marion Gehlen, Tatiana Ilyina, and Jasmin G John.
17 2020. 'Twenty-first century ocean warming, acidification, deoxygenation, and upper-
18 ocean nutrient and primary production decline from CMIP6 model projections',
19 *Biogeosciences*, 17: 3439-70.
- 20 Lachkar, Zouhair, Marina Lévy, and K Shafer Smith. 2019. 'Strong intensification of the Arabian
21 Sea oxygen minimum zone in response to Arabian Gulf warming', *Geophysical Research*
22 *Letters*, 46: 5420-29.
- 23 Lachkar, Zouhair, Marina Lévy, and Shafer Smith. 2018. 'Intensification and deepening of the
24 Arabian Sea oxygen minimum zone in response to increase in Indian monsoon wind
25 intensity', *Biogeosciences*, 15: 159-86.
- 26 Lachkar, Zouhair, Michael Mehari, Muchamad Al Azhar, Marina Lévy, and Shafer Smith. 2020.
27 'Fast local warming of sea-surface is the main factor of recent deoxygenation in the
28 Arabian Sea', *Biogeosciences Discussions*: 1-27.
- 29 Lachkar, Zouhair, Shafer Smith, Marina Lévy, and Olivier Pauluis. 2016. 'Eddies reduce
30 denitrification and compress habitats in the Arabian Sea', *Geophysical Research Letters*,
31 43: 9148-56.
- 32 Lévy, Marina, Laure Resplandy, Jaime B Palter, Damien Couespel, and Zouhair Lachkar. 2021.
33 "The crucial contribution of mixing to present and future ocean oxygen distribution." In.:
34 Elsevier.
- 35 Luyten, JR, Joseph Pedlosky, and Henry Stommel. 1983. 'The ventilated thermocline', *Journal of*
36 *Physical Oceanography*, 13: 292-309.
- 37 McCartney, M. S. 1979. 'Subantarctic mode water', *Woods Hole Oceanographic Institution*
38 *Contribution*, 3773: 103-19.

- 1 McClanahan, T. R., M. Ateweberhan, N. A. J. Graham, S. K. Wilson, C. R. Sebastian, M. M. M.
2 Guillaume, and J. H. Bruggemann. 2007. 'Western Indian Ocean coral communities:
3 bleaching responses and susceptibility to extinction', *Marine Ecology Progress Series*,
4 337: 1-13.
- 5 McCreary, J. P., Z. Yu, R. R. Hood, P. N. Vinayachandran, R. Furue, A. Ishida, and K. J.
6 Richards. 2013. 'Dynamics of the Indian-Ocean oxygen minimum zones', *Progress in*
7 *Oceanography*, 112-113: 15-37.
- 8 McElroy, MB. 1983. 'Marine biological controls on atmospheric CO₂ and climate', *Nature*, 302:
9 328-29.
- 10 Moore, J. A., L. M. Bellchambers, M. R. Depczynski, R. D. Evans, S. N. Evans, S. N. Field, K.
11 J. Friedman, J. P. Gilmour, T. H. Holmes, R. Middlebrook, B. T. Radford, T. Ridgway,
12 G. Shedrawi, H. Taylor, D. P. Thompson, and S. K. Wilson. 2012. 'Unprecedented mass
13 bleaching and loss of coral across 12 degrees of latitude in Western Australia in 2010-11',
14 *PloS ONE*, 7: e51087, doi:10.1317/journal.pone.0051807.
- 15 Moore, Willard S. 1984. 'Review of the geosecs project', *Nuclear Instruments and Methods in*
16 *Physics Research*, 223: 459-65.
- 17 Morrison, J. M., L. A. Codispoti, S. L. Smith, K. Wishner, C. Flagg, W. D. Gardner, S. Gaurin,
18 S. W. A. Naqvi, V. Manghnani, L. Prosperie, and J. S. Gundersen. 1999. 'The oxygen
19 minimum zone in the Arabian Sea during 1995', *Deep-Sea Research (Part II, Topical*
20 *Studies in Oceanography)*, 46: 1903-31.
- 21 Naqvi, S Wajih A, Ronald J Noronha, and CV Gangadhara Reddy. 1982. 'Denitrification in the
22 Arabian Sea', *Deep Sea Research Part A. Oceanographic Research Papers*, 29: 459-69.
- 23 Naqvi, S. W. A. 1991. 'Geographical extent of denitrification in the Arabian Sea in relation to
24 some physical processes', *Oceanologica Acta*, 14: 281-90.
- 25 ———. 2019. 'Evidence for ocean deoxygenation and its patterns: Indian Ocean', *Ocean*
26 *deoxygenation: Everyone's problem*, edited by: Laffoley, D. and Baxter, JM, IUCN,
27 Gland, Switzerland.
- 28 Naqvi, S. W. A., H. W. Bange, S. W. Gibb, C. Goyet, A. D. Hatton, and R. C. Upstill-Goddard.
29 2005. 'Biogeochemical ocean-atmosphere transfers in the Arabian Sea', *Progress in*
30 *Oceanography*, 65: 116-44.
- 31 Naqvi, S. W. A., D. A. Jayakumar, P. V. Narvekar, H. Naik, Vvss Sarma, W. D'Souza, S. Joseph,
32 and M. D. George. 2000. 'Increased marine production of N₂O due to intensifying anoxia
33 on the Indian continental shelf', *Nature*, 408: 346-49.
- 34 Newell, BS. 1969. 'Seasonal variations in the Indian Ocean along 110° E. II. Particulate carbon',
35 *Marine and Freshwater Research*, 20: 51-54.
- 36 Obura, David, Mishal Gudka, F Abdou Rabi, S Bacha Gian, L Bigot, J Bijoux, S Freed, J
37 Maharavo, V Munbodhe, and J Mwaura. 2017. 'Coral reef status report for the Western
38 Indian Ocean. Global Coral Reef Monitoring Network (GCRMN)', *International Coral*
39 *Reef Initiative (ICRI)*, 144.

- 1 Paulmier, Aurélien, and Diana Ruiz-Pino. 2009. 'Oxygen minimum zones (OMZs) in the modern
2 ocean', *Progress in Oceanography*, 80: 113-28.
- 3 Pazan, Stephen E, and Peter Niiler. 2004. "New global drifter data set available." In.: Wiley
4 Online Library.
- 5 Piketh, S. J. , P. D. Tyson, and W. Steffen. 2000. 'Aeolian transport from southern Africa and
6 iron fertilization of marine biota in the South Indian Ocean', *South African Journal of
7 Science*, 96: 244-46.
- 8 Piontkovski, SA, and HS Al-Oufi. 2015. 'The Omani shelf hypoxia and the warming Arabian
9 Sea', *International Journal of Environmental Studies*, 72: 256-64.
- 10 Queste, Bastien Y, Clément Vic, Karen J Heywood, and Sergey A Piontkovski. 2018. 'Physical
11 controls on oxygen distribution and denitrification potential in the north west Arabian
12 Sea', *Geophysical Research Letters*, 45: 4143-52.
- 13 Ramaswamy, V, RR Nair, SI Manganini, B Haake, and V Ittekkot. 1991. 'Lithogenic fluxes to
14 the deep Arabian Sea measured by sediment traps', *Deep Sea Research Part A*.
15 *Oceanographic Research Papers*, 38: 169-84.
- 16 Ramaswamy, V., O. Boucher, J. Haigh, D. Hauglustaine, J. Haywood, G. Myhre, T. Nakajima,
17 G. Y. Shi, and S. Solomon. 2001. 'Radiative Forcing of Climate Change.' in J. T.
18 Houghton, Y. Ding, Griggs, D. J., M. Noguer, P. J. Van der Linden, X. Dai, K. Maskell
19 and C. A. Johnson (eds.), *Climate Change 2001: The Scientific Basis: Contribution of
20 Working Group I to the Third Assessment Report of the Intergovernmental Panel on
21 Climate Change* (Cambridge University Press: Cambridge, U. K.).
- 22 Rao, CK, SWA Naqvi, M Dileep Kumar, SJD Varaprasad, DA Jayakumar, MD George, and
23 SYS Singbal. 1994. 'Hydrochemistry of the Bay of Bengal: possible reasons for a
24 different water-column cycling of carbon and nitrogen from the Arabian Sea', *Marine
25 Chemistry*, 47: 279-90.
- 26 Rao, DN, M Chopra, GR Rajula, DSL Durgadevi, and VVSS Sarma. 2021. 'Release of
27 significant fraction of primary production as dissolved organic carbon in the Bay of
28 Bengal', *Deep Sea Research Part I: Oceanographic Research Papers*, 168: 103445.
- 29 Rao, DN, and VVSS Sarma. 2022. 'Accumulation of dissolved organic carbon and nitrogen in
30 the photic zone in the nitrogen-depleted waters of the Bay of Bengal', *Marine Chemistry*,
31 239: 104074.
- 32 Rashid, T., S. Hoque, and F. Akter. 2013. 'Ocean acidification in the Bay of Bengal', *Scientific
33 Reports*, 2: 699.
- 34 Resplandy, Laure. 2018. 'Climate change and oxygen in the ocean', *Nature: International Weekly
35 Journal of Science*.
- 36 Resplandy, Laure, Marina Lévy, Laurent Bopp, Vincent Echevin, Stéphane Pous, VVSS Sarma,
37 and D Kumar. 2012. 'Controlling factors of the oxygen balance in the Arabian Sea's
38 OMZ', *Biogeosciences*, 9: 5095-109.

- 1 Rixen, Tim, Antje Baum, Birgit Gaye, and Birgit Nagel. 2014. 'Seasonal and interannual
2 variations in the nitrogen cycle in the Arabian Sea', *Biogeosciences*, 11: 5733-47.
- 3 Rixen, Tim, Greg Cowie, Birgit Gaye, Joaquim Goes, Helga do Rosário Gomes, Raleigh R
4 Hood, Zouhair Lachkar, Henrike Schmidt, Joachim Segschneider, and Arvind Singh.
5 2020. 'Reviews and syntheses: Present, past, and future of the oxygen minimum zone in
6 the northern Indian Ocean', *Biogeosciences*, 17: 6051-80.
- 7 Rixen, Tim, Birgit Gaye, and Kay-Christian Emeis. 2019a. 'The monsoon, carbon fluxes, and the
8 organic carbon pump in the northern Indian Ocean', *Progress in Oceanography*, 175: 24-
9 39.
- 10 Rixen, Tim, Birgit Gaye, Kay-Christian Emeis, and Venkitasubramani Ramaswamy. 2019b. 'The
11 ballast effect of lithogenic matter and its influences on the carbon fluxes in the Indian
12 Ocean', *Biogeosciences*, 16: 485-503.
- 13 Rixen, Tim, and Venugopalan Ittekkot. 2005. 'Nitrogen deficits in the Arabian Sea, implications
14 from a three component mixing analysis', *Deep Sea Research Part II: Topical Studies in
15 Oceanography*, 52: 1879-91.
- 16 Sarma, V. V. S. S., A. Lenton, R. M. Law, N. Metzl, P. K. Patra, S. Doney, I. D. Lima, E.
17 Dlugokencky, M. Ramonet, and V. Valsala. 2013. 'Sea-air CO₂ fluxes in the Indian
18 Ocean between 1990 and 2009', *Biogeosciences*, 10: 7035-52.
- 19 Sarma, VVSS, TVS Udaya Bhaskar, J Pavan Kumar, and Kunal Chakraborty. 2020. 'Potential
20 mechanisms responsible for occurrence of core oxygen minimum zone in the north-
21 eastern Arabian Sea', *Deep Sea Research Part I: Oceanographic Research Papers*, 165:
22 103393.
- 23 Sarma, VVSS, L Jagadeesan, HB Dalabehera, DN Rao, GS Kumar, DS Durgadevi, K Yadav, S
24 Behera, and MMR Priya. 2018. 'Role of eddies on intensity of oxygen minimum zone in
25 the Bay of Bengal', *Continental Shelf Research*, 168: 48-53.
- 26 Sarma, VVSS, MS Krishna, YS Paul, and VSN Murty. 2015a. 'Observed changes in ocean
27 acidity and carbon dioxide exchange in the coastal Bay of Bengal—a link to air pollution',
28 *Tellus B: Chemical and Physical Meteorology*, 67: 24638.
- 29 Sarma, VVSS, MS Krishna, VD Rao, R Viswanadham, NA Kumar, TR Kumari, L Gawade, S
30 Ghatkar, and A Tari. 2012. 'Sources and sinks of CO₂ in the west coast of Bay of
31 Bengal', *Tellus B: Chemical and Physical Meteorology*, 64: 10961.
- 32 Sarma, VVSS, MS Krishna, TNR Srinivas, VR Kumari, K Yadav, and MD Kumar. 2021.
33 'Elevated acidification rates due to deposition of atmospheric pollutants in the coastal
34 Bay of Bengal', *Geophysical Research Letters*, 48: e2021GL095159.
- 35 Sarma, VVSS, JS Patil, D Shankar, and AC Anil. 2019. 'Shallow convective mixing promotes
36 massive Noctiluca scintillans bloom in the northeastern Arabian Sea', *Marine Pollution
37 Bulletin*, 138: 428-36.
- 38 Sarma, VVSS, YS Paul, DG Vani, and VSN Murty. 2015. 'Impact of river discharge on the
39 coastal water pH and pCO₂ levels during the Indian Ocean Dipole (IOD) years in the
40 western Bay of Bengal', *Continental Shelf Research*, 107: 132-40.

- 1 Sarma, VVSS, and TVS Udaya Bhaskar. 2018. 'Ventilation of oxygen to oxygen minimum zone
2 due to anticyclonic eddies in the Bay of Bengal', *Journal of Geophysical Research:
3 Biogeosciences*, 123: 2145-53.
- 4 Sathyendranath, Shubha, Venetia Stuart, Anitha Nair, Kenji Oka, Toru Nakane, Heather
5 Bouman, Marie-Hélène Forget, Heidi Maass, and Trevor Platt. 2009. 'Carbon-to-
6 chlorophyll ratio and growth rate of phytoplankton in the sea', *Marine Ecology Progress
7 Series*, 383: 73-84.
- 8 Schmidt, Henrike, Rena Czeschel, and Martin Visbeck. 2020. 'Seasonal variability of the
9 circulation in the Arabian Sea at intermediate depth and its link to the Oxygen Minimum
10 Zone', *Ocean Science Discussions*.
- 11 Schmidt, Henrike, Julia Getzlaff, Ulrike Löptien, and Andreas Oschlies. 2021. 'Causes of
12 uncertainties in the representation of the Arabian Sea oxygen minimum zone in CMIP5
13 models', *Ocean Science Discussions*: 1-32.
- 14 Schmidtko, Sunke, Lothar Stramma, and Martin Visbeck. 2017. 'Decline in global oceanic
15 oxygen content during the past five decades', *Nature*, 542: 335-39.
- 16 Schunck, Harald, Gaute Lavik, Dhvani K Desai, Tobias Großkopf, Tim Kalvelage, Carolin R
17 Löscher, Aurélien Paulmier, Sergio Contreras, Herbert Siegel, and Moritz Holtappels.
18 2013. 'Giant hydrogen sulfide plume in the oxygen minimum zone off Peru supports
19 chemolithoautotrophy', *PloS ONE*, 8: e68661.
- 20 Schwartz, Matthew C, Clare Woulds, and Gregory L Cowie. 2009. 'Sedimentary denitrification
21 rates across the Arabian Sea oxygen minimum zone', *Deep Sea Research Part II: Topical
22 Studies in Oceanography*, 56: 324-32.
- 23 Seiwel, Harry Richard. 1937. *The minimum oxygen concentration in the western basin of the
24 North Atlantic* (Massachusetts Institute of Technology).
- 25 SenGupta, R., and S. W. A. Naqvi. 1984. 'Chemical oceanography of the Indian Ocean, north of
26 the equator', *Deep Sea Research Part A. Oceanographic Research Papers*, 31: 671-706.
- 27 Sewell, R. B. S. . 1934. 'The John Murray Expedition to the Arabian Sea', *Nature*, 133: 669-72.
- 28 SEWELL, RB SEYMOUR, and Louis Fage. 1948. 'Minimum oxygen layer in the ocean', *Nature*,
29 162: 949-51.
- 30 Shah, Chinmay, AK Sudheer, and Ravi Bhushan. 2018. 'Distribution of dissolved organic carbon
31 in the Bay of Bengal: Influence of sediment discharge, fresh water flux, and productivity',
32 *Marine Chemistry*, 203: 91-101.
- 33 Somasundar, K, A Rajendran, M Dileep Kumar, and R Sen Gupta. 1990. 'Carbon and nitrogen
34 budgets of the Arabian Sea', *Marine Chemistry*, 30: 363-77.
- 35 Somes, Christopher J, Andreas Oschlies, and A Schmittner. 2013. 'Isotopic constraints on the
36 pre-industrial oceanic nitrogen budget', *Biogeosciences*, 10: 5889-910.

- 1 Sredivi, B., and V. V. S. S. Sarma (2022) 'Enhanced Atmospheric pollutants strengthened winter
2 convective mixing and phytoplankton blooms in the northern Arabian Sea', *Journal of*
3 *Geophysical Research, Biogeosciences*, 127, e2021JG006527.
- 4 Sreeush, Mohanan Geethalekshmi, Saran Rajendran, Vinu Valsala, Sreenivas Pentakota, KVSR
5 Prasad, and Raghu Murtugudde. 2019. 'Variability, trend and controlling factors of Ocean
6 acidification over Western Arabian Sea upwelling region', *Marine Chemistry*, 209: 14-24.
- 7 Sreeush, Mohanan Geethalekshmi, Vinu Valsala, Sreenivas Pentakota, Koneru Venkata Siva
8 Rama Prasad, and Raghu Murtugudde. 2018. 'Biological production in the Indian Ocean
9 upwelling zones–Part 1: refined estimation via the use of a variable compensation depth
10 in ocean carbon models', *Biogeosciences*, 15: 1895-918.
- 11 Sreeush, Mohanan Geethalekshmi, Vinu Valsala, Halder Santanu, Sreenivas Pentakota, KVSR
12 Prasad, CV Naidu, and Raghu Murtugudde. 2020. 'Biological production in the Indian
13 Ocean upwelling zones-Part 2: Data based estimates of variable compensation depth for
14 ocean carbon models via cyclo-stationary Bayesian Inversion', *Deep Sea Research Part*
15 *II: Topical Studies in Oceanography*, 179: 104619.
- 16 Sridevi, B, and VVSS Sarma. 2021. 'Role of river discharge and warming on ocean acidification
17 and pCO₂ levels in the Bay of Bengal', *Tellus B: Chemical and Physical Meteorology*,
18 73: 1-20.
- 19 Stramma, L., G. C. Johnson, J. Sprintall, and V. Mohrholz. 2008. 'Expanding oxygen-minimum
20 zones in the tropical oceans,' *Science*, 320: 655-58.
- 21 Stramma, L., S. Schmidtko, L. A. Levin, and G. C. Johnson. 2010. 'Ocean oxygen minima
22 expansions and their biological impacts', *Deep-Sea Research, Part I*, 57: 587-95.
- 23 Strutton, P. G., V. J. Coles, R. R. Hood, R. J. Matear, M. J. McPhaden, and H. E. Phillips. 2015.
24 'Biogeochemical variability in the central equatorial Indian Ocean during the monsoon
25 transition', *Biogeosciences*, 12: 2367-82.
- 26 Subha Anand, S , R Rengarajan, Damodar Shenoy, Mangesh Gauns, and SWA Naqvi. 2018b.
27 'POC export fluxes in the Arabian Sea and the Bay of Bengal: A simultaneous
28 ²³⁴Th/²³⁸U and ²¹⁰Po/²¹⁰Pb study', *Marine Chemistry*, 198: 70-87.
- 29 Subha Anand, S, R Rengarajan, and VVSS Sarma. 2018a. '²³⁴Th-based carbon export flux along
30 the Indian GEOTRACES GI02 section in the Arabian Sea and the Indian Ocean', *Global*
31 *Biogeochemical Cycles*, 32: 417-36.
- 32 Subha Anand, S, R Rengarajan, VVSS Sarma, AK Sudheer, R Bhushan, and SK Singh. 2017.
33 'Spatial variability of upper ocean POC export in the Bay of Bengal and the Indian O
34 cean determined using particle-reactive ²³⁴Th', *Journal of Geophysical Research:*
35 *Oceans*, 122: 3753-70.
- 36 Sudheesh, V, GVM Gupta, KV Sudharma, H Naik, DM Shenoy, M Sudhakar, and SWA Naqvi.
37 2016. 'Upwelling intensity modulates N₂O concentrations over the western Indian shelf',
38 *Journal of Geophysical Research: Oceans*, 121: 8551-65.
- 39 Sverdrup, H. U. , M. W. Johnson, and R. H. Fleming. 1942. *The Oceans: Their Physics,*
40 *Chemistry and General Biology* (Prentice-Hall: Englewood Cliffs, N.J.).

- 1 Sverdrup, HU. 1938. 'On the explanation of the oxygen minima and maxima in the oceans', *ICES*
2 *Journal of Marine Science*, 13: 163-72.
- 3 Swallow, J. . 1984. 'Some aspects of the physical oceanography of the Indian Ocean', *Deep Sea*
4 *Research*, 31: 639-50.
- 5 Takahashi, T., and et al. 2009. 'Climatological mean and decadal change in surface ocean pCO₂,
6 and net sea-air CO₂ flux over the global ocean', *Deep-Sea Research, part II*, 56: 554-77.
- 7 Takahashi, T., S.C. Sutherland, D. Chipman, J. G. Goddard, C. Ho, T. Newberger, C. Sweeney,
8 and D. R. Munro. 2014. 'Climatological distributions of pH, pCO₂, total CO₂, alkalinity,
9 and CaCO₃ saturationh in the global surface ocean, and temporal changes at selected
10 locations', *Marine Chemistry*, 164: 95-125.
- 11 Takahashi, T., S.C. Sutherland, C. Sweeney, A. Poisson, N. Metzl, B. Tilbrook, N. Bates, R.
12 Wanninkhof, R.A. Feely, C. Sabine, J. Olafsson, and Y. Nojiri. 2002. 'Global sea-air CO₂
13 flux based on climatological surface ocean pCO₂, and seasonal biological and
14 temperature effects', *Deep-Sea Research Part II*, 49: 1601-23.
- 15 Talley, Lynne D, Gregory C Johnson, Sarah Purkey, Richard A Feely, and Rik Wanninkhof.
16 2017. "Global Ocean Ship-based Hydrographic Investigations Program (GO-SHIP)
17 provides key climate-relevant deep ocean observations, US CLIVAR Variations, 15." In.
- 18 Tarique, Mohd, Waliur Rahaman, AA Fousiya, N Lathika, Meloth Thamban, Hema Achyuthan,
19 and Sambuddha Misra. 2021. 'Surface pH Record (1990–2013) of the Arabian Sea From
20 Boron Isotopes of Lakshadweep Corals—Trend, Variability, and Control', *Journal of*
21 *Geophysical Research: Biogeosciences*, 126: e2020JG006122.
- 22 Tchernia, Paul. 1980. 'Descriptive regional oceanography'.
- 23 Thushara, Venugopal, Puthenveetil Narayana Menon Vinayachandran, Adrian J Matthews,
24 Benjamin GM Webber, and Bastien Y Queste. 2019. 'Vertical distribution of chlorophyll
25 in dynamically distinct regions of the southern Bay of Bengal', *Biogeosciences*, 16: 1447-
26 68.
- 27 Udaya Bhaskar, TVS, VVSS Sarma, and J Pavan Kumar. 2021. 'Potential mechanisms
28 responsible for spatial variability in intensity and thickness of oxygen minimum zone in
29 the Bay of Bengal', *Journal of Geophysical Research: Biogeosciences*, 126:
30 e2021JG006341.
- 31 Vallivattathillam, Parvathi, Suresh Iyyappan, Matthieu Lengaigne, Christian Ethé, Jérôme
32 Vialard, Marina Levy, Neetu Suresh, Olivier Aumont, Laure Resplandy, and Hema Naik.
33 2017. 'Positive Indian Ocean Dipole events prevent anoxia off the west coast of India',
34 *Biogeosciences*, 14: 1541-59.
- 35 Valsala, V., S. Maksyutov, and R. Murtugudde. 2012. 'A window for carbon uptake in the
36 southern subtropical Indian Ocean', *Geophysical Research Letters*, 39: L17605.
- 37 Valsala, Vinu. 2009. 'Different spreading of Somali and Arabian coastal upwelled waters in the
38 northern Indian Ocean: A case study', *Journal of Oceanography*, 65: 803-16.

- 1 Valsala, Vinu, and Shamil Maksyutov. 2010. 'Simulation and assimilation of global ocean pCO₂
2 and air–sea CO₂ fluxes using ship observations of surface ocean pCO₂ in a simplified
3 biogeochemical offline model', *Tellus B: Chemical and Physical Meteorology*, 62: 821-
4 40.
- 5 ———. 2013. 'Interannual variability of the air–sea CO₂ flux in the north Indian Ocean', *Ocean
6 Dynamics*, 63: 165-78.
- 7 Valsala, Vinu, and Raghu Murtugudde. 2015. 'Mesoscale and intraseasonal air–sea CO₂
8 exchanges in the western Arabian Sea during boreal summer', *Deep Sea Research Part I:
9 Oceanographic Research Papers*, 103: 101-13.
- 10 Valsala, Vinu, MG Sreeush, and Kunal Chakraborty. 2020. 'The IOD impacts on the Indian
11 Ocean Carbon cycle', *Journal of Geophysical Research: Oceans*, 125: e2020JC016485.
- 12 Valsala, Vinu, Mohanan Geethalekshmi Sreeush, M Anju, Pentakota Sreenivas, Yogesh K
13 Tiwari, Kunal Chakraborty, and S Sijikumar. 2021. 'An observing system simulation
14 experiment for Indian Ocean surface pCO₂ measurements', *Progress in Oceanography*,
15 194: 102570.
- 16 Vaquer-Sunyer, Raquel, and Carlos M Duarte. 2008. 'Thresholds of hypoxia for marine
17 biodiversity', *Proceedings of the National Academy of Sciences*, 105: 15452-57.
- 18 Vinayachandran, P. N. 2009. 'Impact of physical processes on chlorophyll distribution in the Bay
19 of Bengal.' in J. D. Wiggert, R. R. Hood, S. W. A. Naqvi, K. H. Brink and S. L. Smith
20 (eds.), *Indian Ocean Biogeochemical Processes and Ecological Variability* (American
21 Geophysical Union: Washington D.C.).
- 22 Volk, T., and M. I. Hoffert. 1985. 'The carbon cycle and atmospheric CO₂, natural variation
23 archean to present', In E.T. Sundquist, W.S. Broecker (Eds.), *The Carbon Cycle and
24 Atmospheric CO₂: Natural Variations Archean to Present, Vol. Geophysical Monograph
25 32 (pp. 99-110). Washington: AGU.*
- 26 Waite, Anya M, Lars Stemann, Lionel Guidi, Paulo HR Calil, Andrew Mc C Hogg, Ming
27 Feng, Peter A Thompson, Marc Picheral, and Gaby Gorsky. 2016. 'The wineglass effect
28 shapes particle export to the deep ocean in mesoscale eddies', *Geophysical Research
29 Letters*, 43: 9791-800.
- 30 Weeks, Scarla J, Bronwen Currie, and Andrew Bakun. 2002. 'Massive emissions of toxic gas in
31 the Atlantic', *Nature*, 415: 493-94.
- 32 Woods, John D. 1985. 'The world ocean circulation experiment', *Nature*, 314: 501-11.

Table 1: Definitions, thresholds, and impacts of different hypoxia thresholds from Hofmann et al 2011.

Terminology	Threshold for impacts to occur maybe in different units	Impacts	Indian Ocean Regions with oxygen minimums below threshold	References
Mild Hypoxia	107 $\mu\text{mol/kg}$, 109 μM , 3.5 mgO_2/l , ~53 % saturation,	Sensitive species show avoidance reactions	Eastern and Central Indian Ocean south of 20S, Western Indian Ocean south of 10S	Cenr 2010
Hypoxia	61 $\mu\text{mol/kg}$, 63 μM , 2 mgO_2/l , ~30 % saturation,	Fishes and the majority of higher organisms suffer from oxygen deficiency, ecosystem adapted to low oxygen conditions	Arabian Sea, Bay of Bengal	Ekau et al., 2010; Vaquer-Sunyer and Duarte 2008
Microbial hypoxia, suboxic, Severe hypoxia, typical OMZ definition.	22 $\mu\text{mol/kg}$, 22 μM , 0.71 mgO_2/l , ~11 % saturation	Microbes start to experience the toxic effects of oxygen on anaerobic processes, only highly specialized species survive	Northern tropical Indian Ocean	Rixen et al., 2020, Diaz and Rosenberg (2008)
Functional anoxia	0.05 μM	Anaerobic microbial processes dominate, nitrite accumulation	Central and Eastern Arabian Sea.	Rixen et al., 2020, Morrison et al., 1999, Ulloa et al, 2012

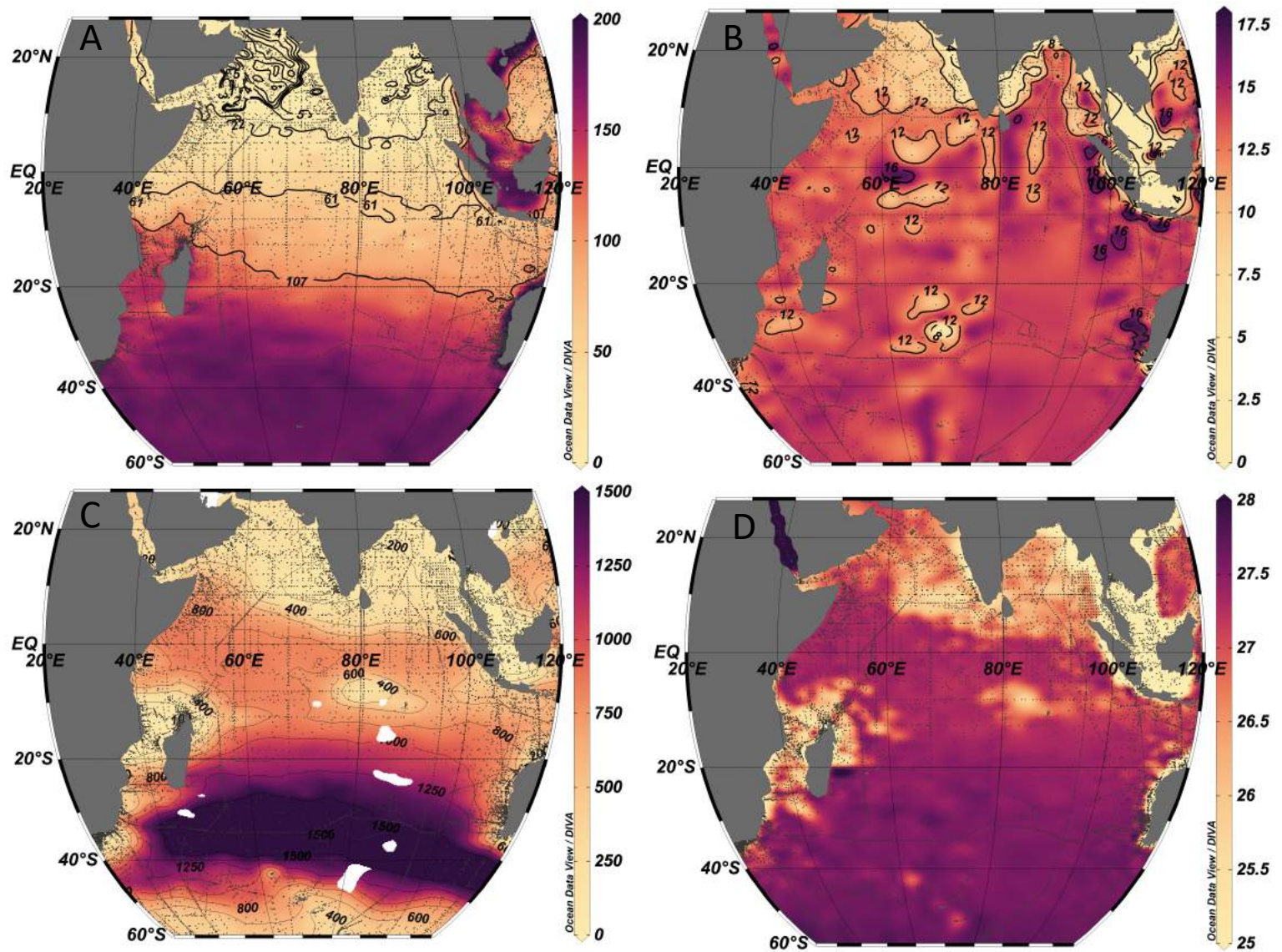


Figure 1: Spatial maps of the A) oxygen concentration (umol/kg) at the depth of the oxygen minimum, B) nitrate to phosphorus ratio at the depth of the oxygen minimum, C) the depth (m) of the oxygen minimum, D) the potential density anomaly (kg/m³) at the depth of the oxygen minimum.

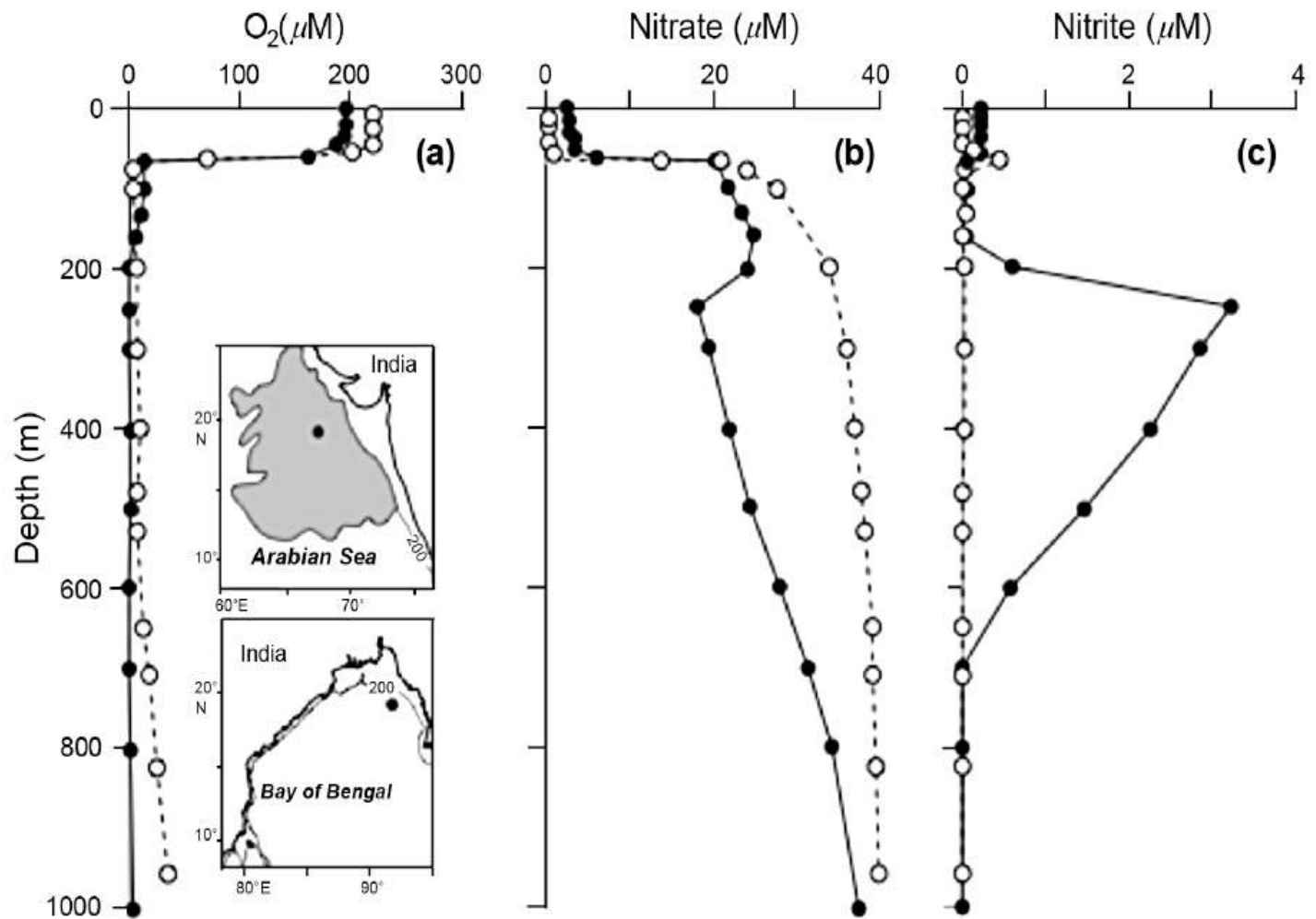


Figure 2: Comparison of vertical profiles of (a) oxygen, (b) nitrate and (c) nitrite in the Arabian Sea (filled circles) and Bay of Bengal (open circles). Station locations are shown in insets. The Arabian Sea inset also shows limit of the denitrification zone to the eastern-central basin. Figure reproduced from Naqvi et al. (2006).

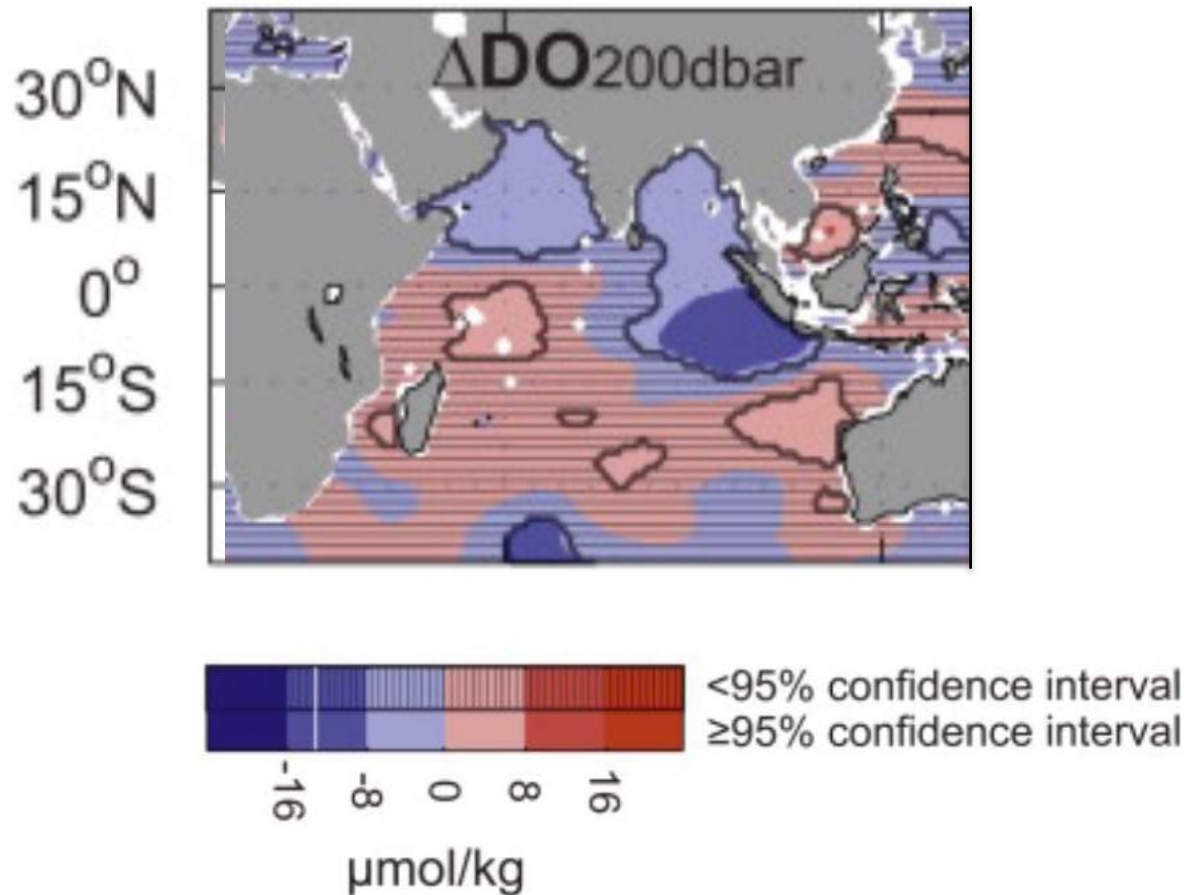


Figure 3: Changes in dissolved oxygen (DO) ($\mu\text{mol kg}^{-1}$) at 200 dbar between 1960–1974 and 1990–2008 in the Indian Ocean. Increases (decreases) in DO are indicated in red (blue). Areas with differences below the 95% confidence interval are shaded by black horizontal lines. Figure modified from Stramma et al. (2010).

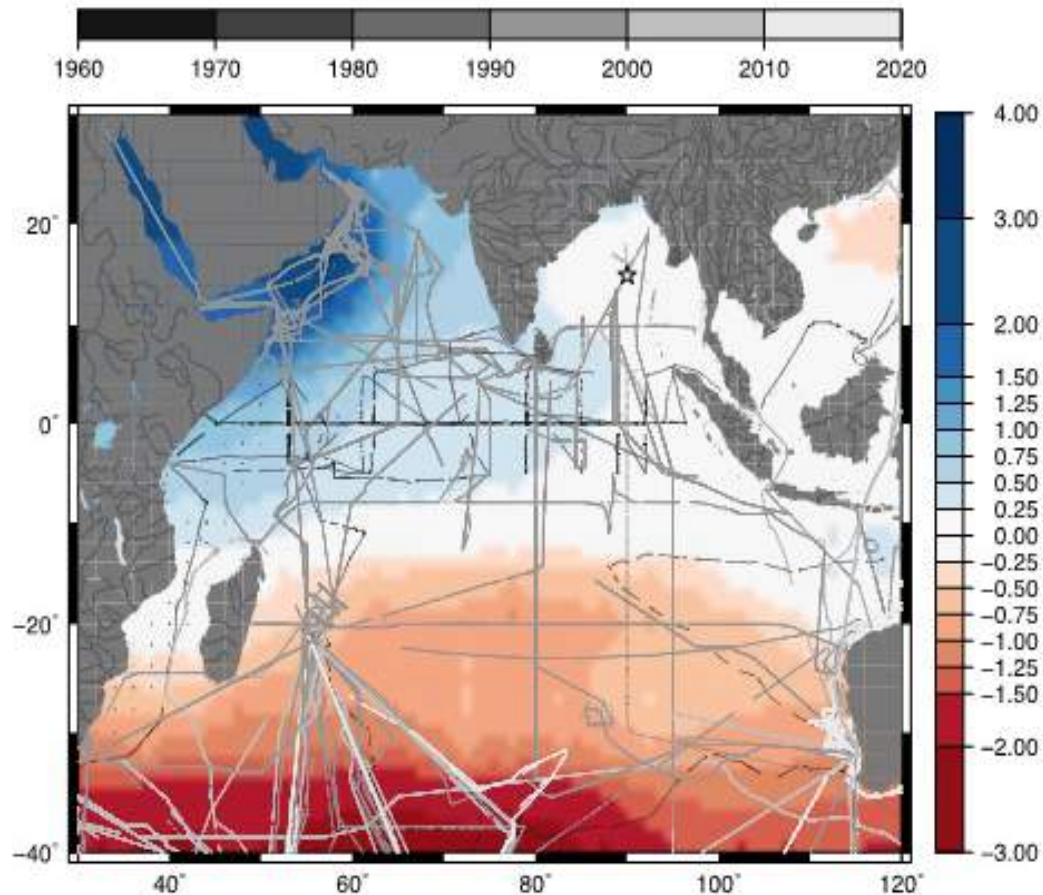


Figure 4: Annual CO₂ flux (mol C m⁻² yr⁻¹) referenced to the year 2000 (Takahashi et al., 2009) over the Indian Ocean. Data points colored by year of collection (Takahashi & Sutherland, 2016) are overlaid as points. Major rivers are also delineated over the continents. The star in the central Bay of Bengal shows the location of a mooring that has been collecting continuous CO₂ and pH measurements since November, 2013. Figure and caption from Hood et al. (2019).

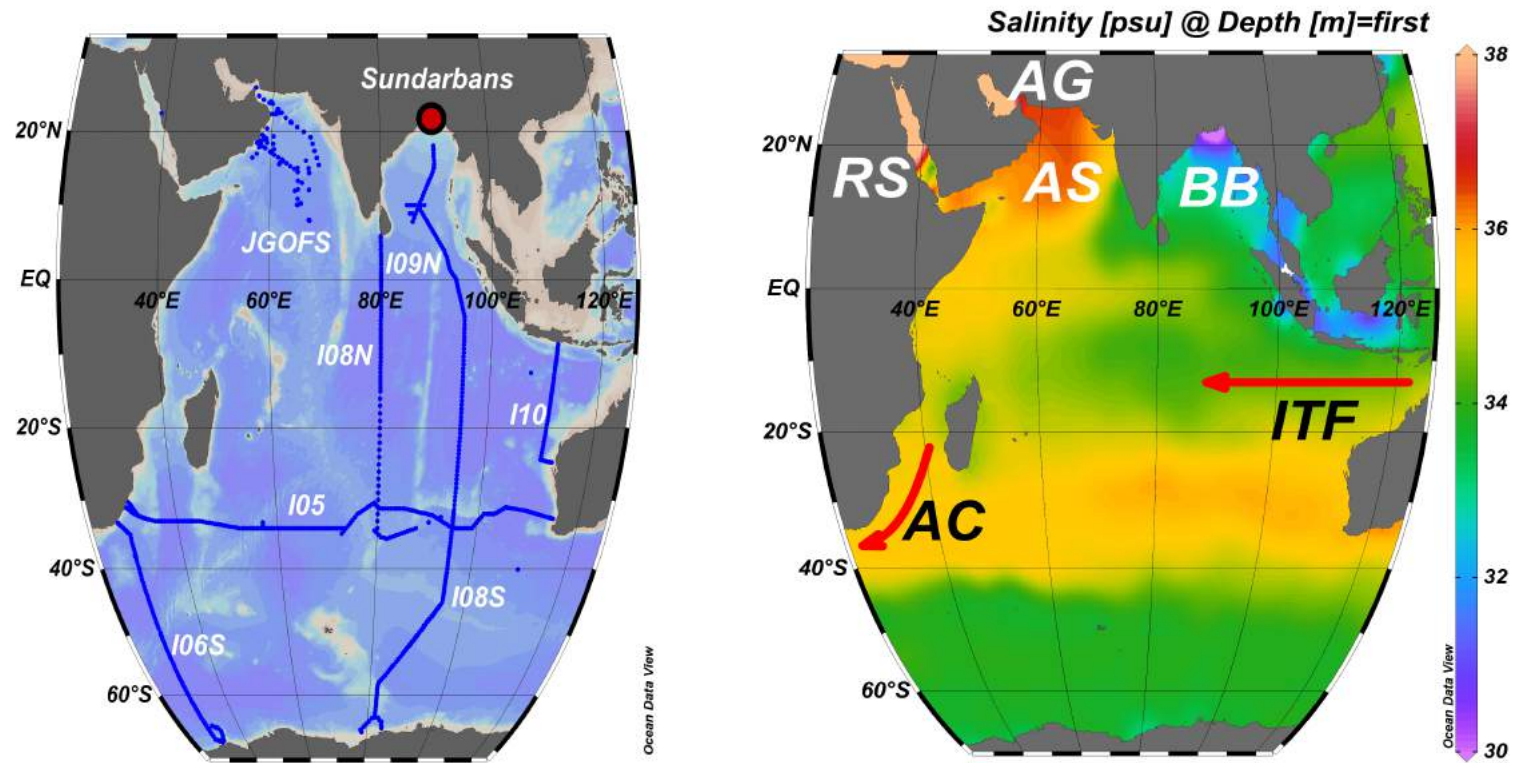


Figure 5: Map of the Indian Ocean showing oceanographic sections discussed (left) and gridded surface salinity (right) during austral summer (WOA), with transports associated with the Indonesian Throughflow (ITF) and Agulhas Current (AC) indicated. Relevant basins are labeled: Arabian Sea (AS); Bay of Bengal (BB); Red Sea (RS); Arabian Gulf (AG), also known as the Persian Gulf.

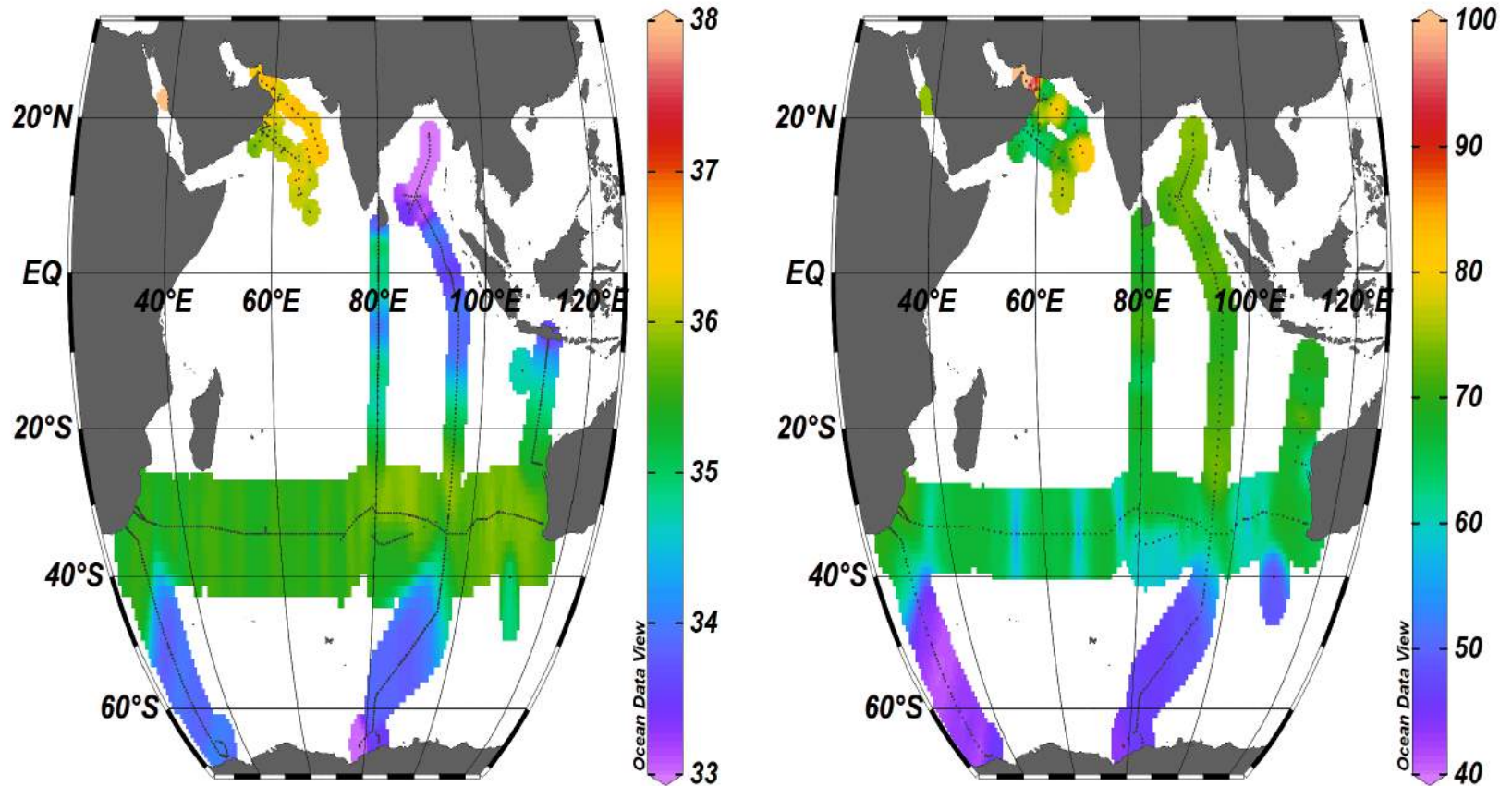


Figure 6: Surface distributions of salinity (left) and DOC ($\mu\text{molC/kg}$; right) observed during cruises. Data from Hansell et al. (2021).

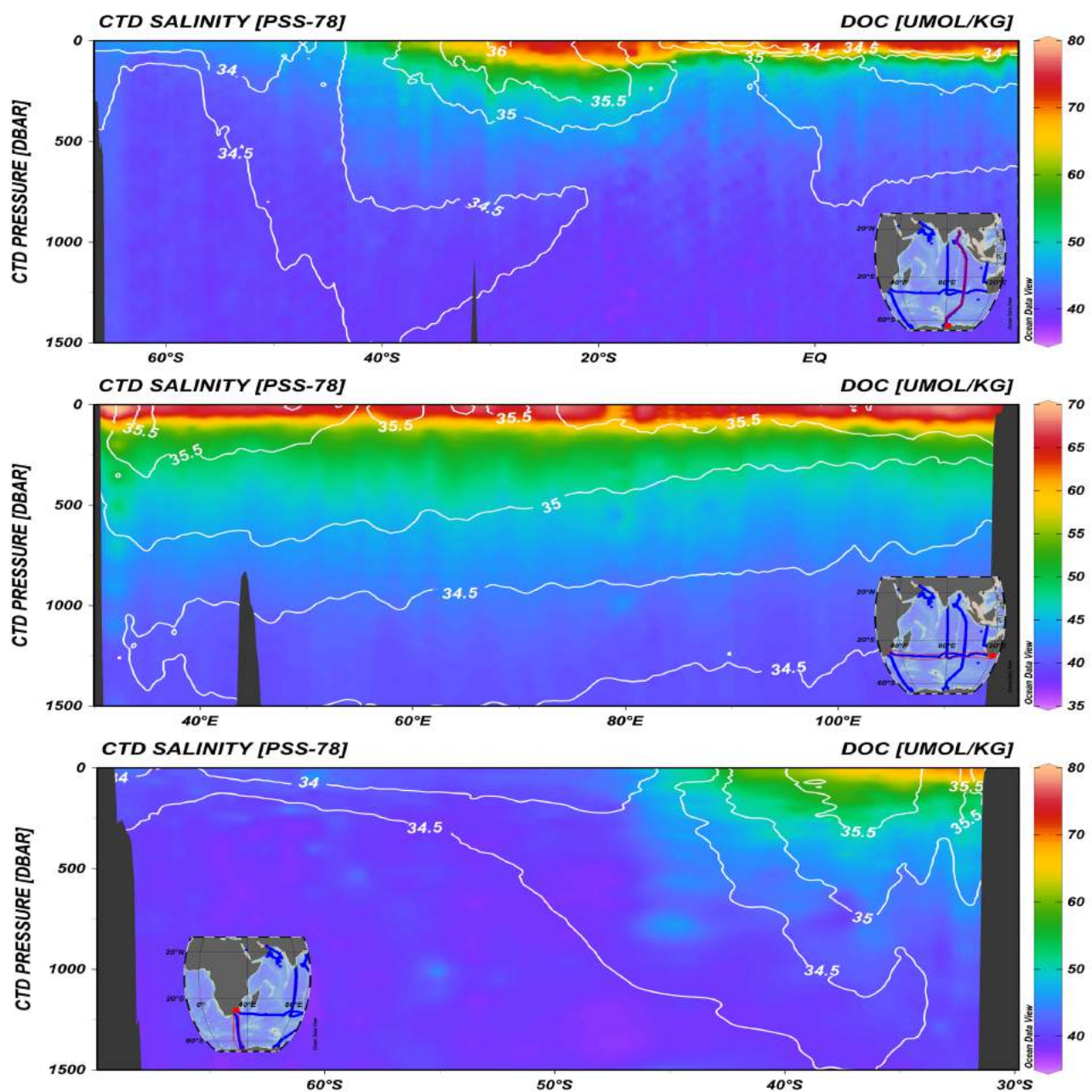


Figure 7: Upper 1500 m section plot of DOC (color; $\mu\text{molC/kg}$) and salinity (contours) along I09N/I08S (top panel, occupied in 2016), I05 (middle panel, occupied in 2009) and I06S (bottom panel, occupied in 2019). Data from Hansell et al. (2021).

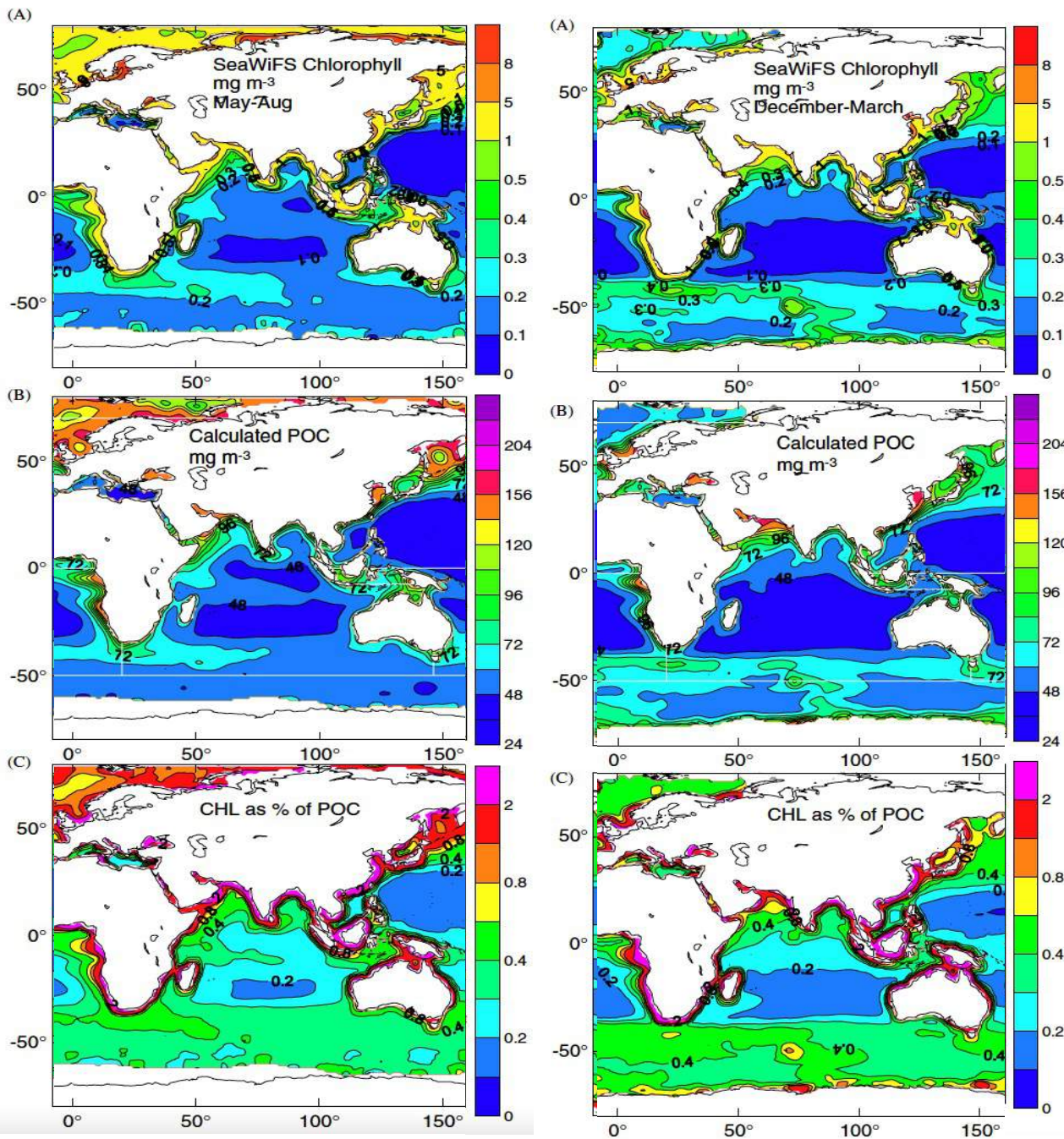


Figure 8: Distribution of: (A) SeaWiFS CHL (mg m^{-3} , level 3, reprocessing 4 data); (B) average POC (mgC m^{-3}) over one attenuation depth calculated from $K_{490}:c_p:\text{POC}$; (C) CHL as a % of POC for: (Left Panels) summer season (1997–2002, May–August, 20 months); (Right Panels) winter season (1997–2002, December–March, 20 months). White lines in (B) mark boundaries separating ocean basins as used by Behrenfeld and Falkowski (1997). Figure and caption modified from Gardner et al. (2006).

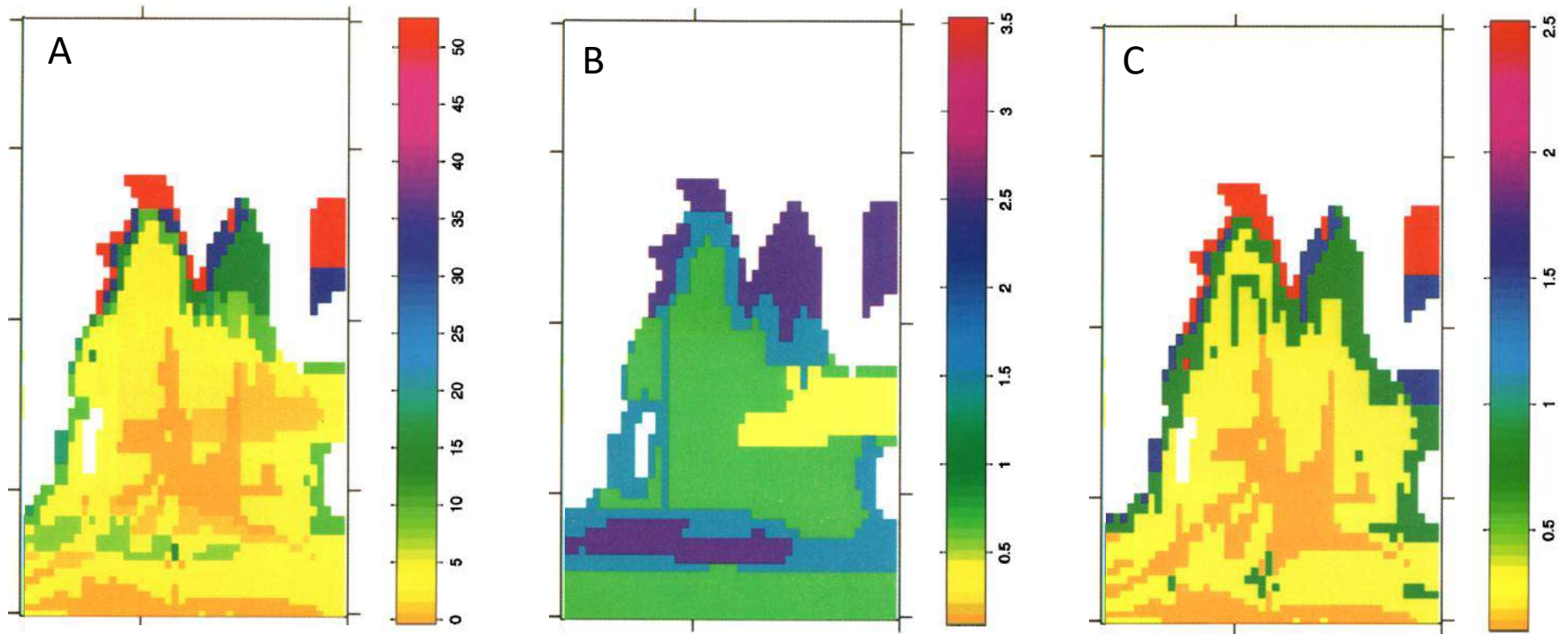


Figure 9: Estimated A) organic carbon burial rate ($\text{mmolC m}^{-2} \text{yr}^{-1}$); B) sediment accumulation rate (grams per square centimeter per thousand years); and C) seafloor distribution of organic carbon (weight percent). Figures and caption modified from Jahnke (1996).

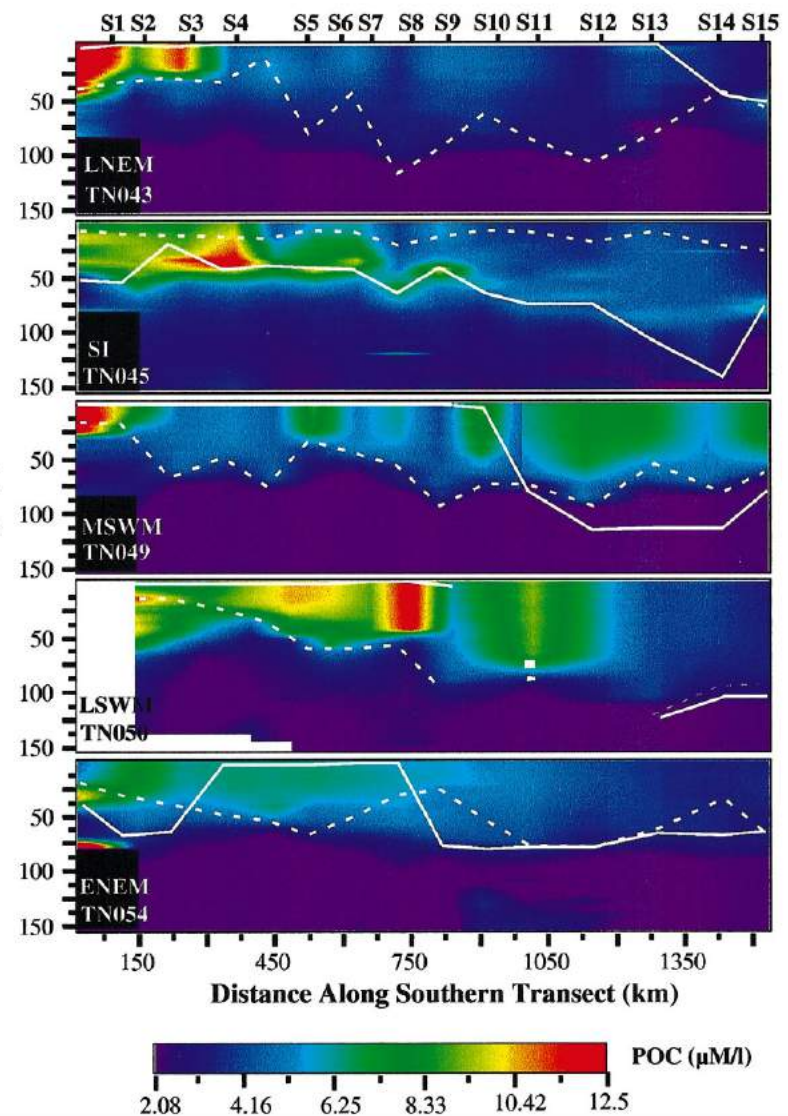
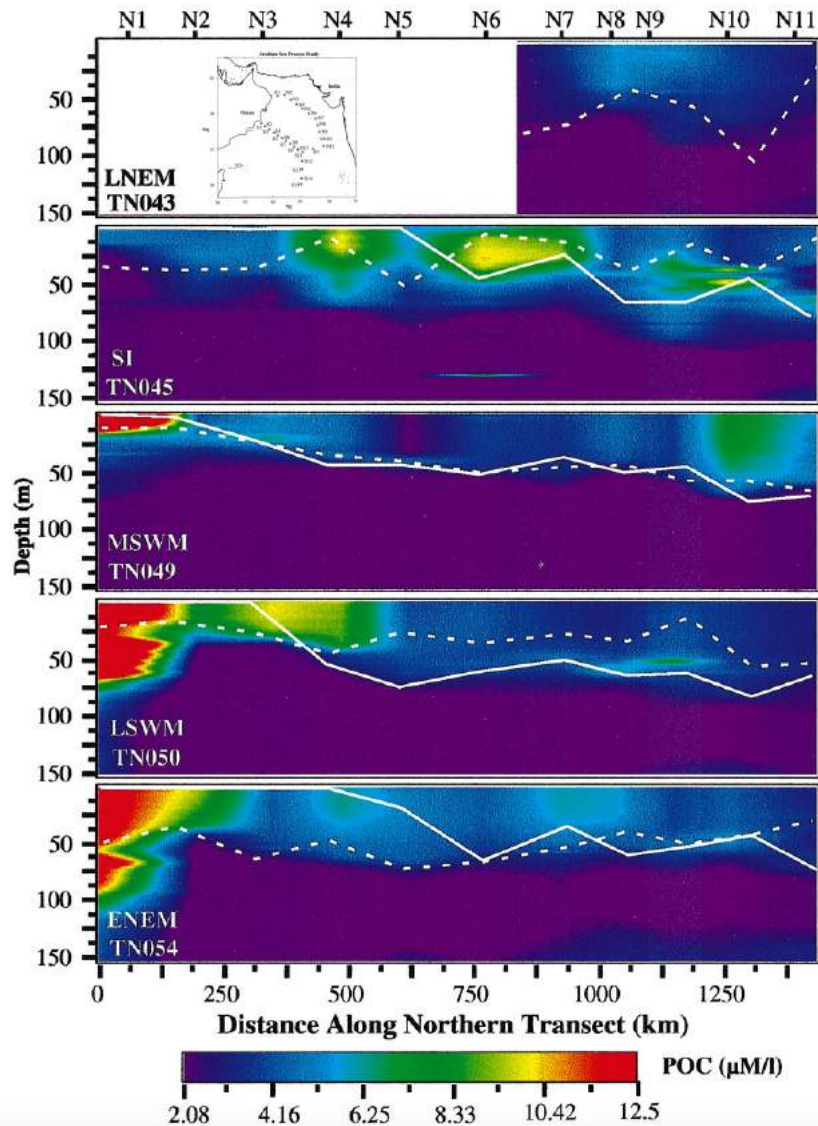


Figure 10: POC sections of the northern transect (left panels) and southern transect (right panels) for each cruise. Mean MLD [$\Delta \sigma = 0.03$] (dotted line) and $0.5 \mu\text{M/l}$ nitrate isopleth (solid line) are shown for each cruise. The station locations are shown in the map inset in the upper left panel. Figures and caption modified from Gunderson et al. (1998).

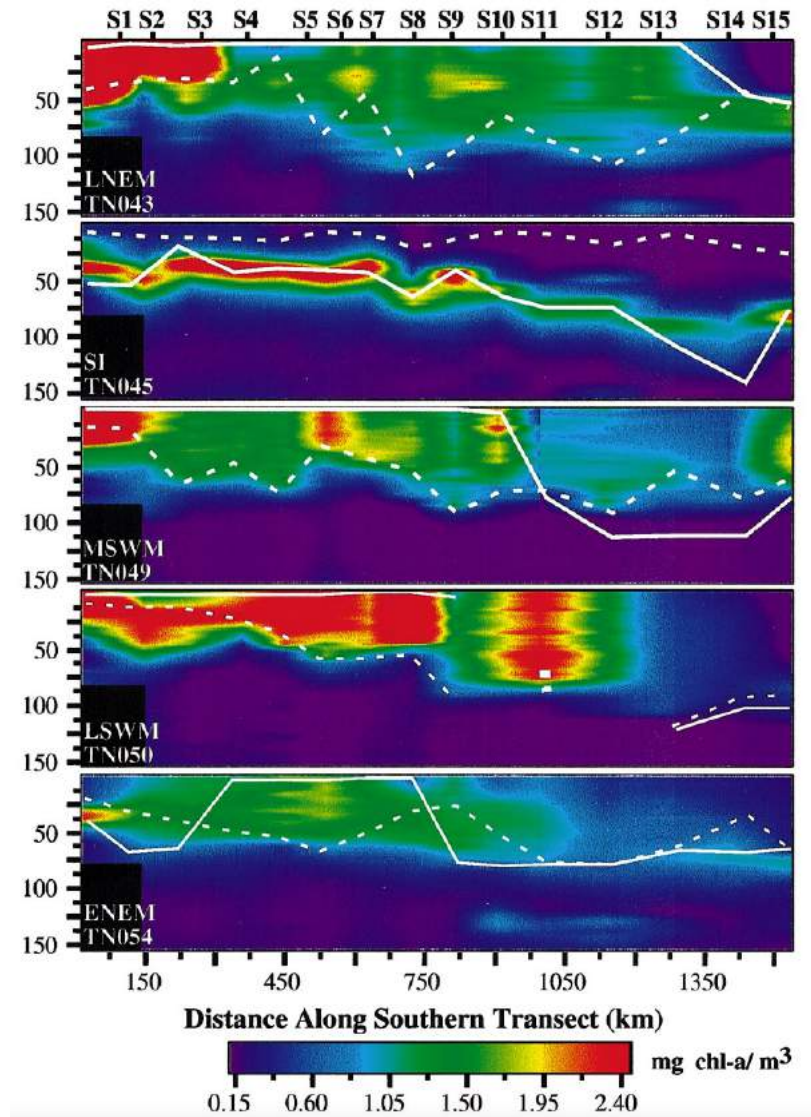
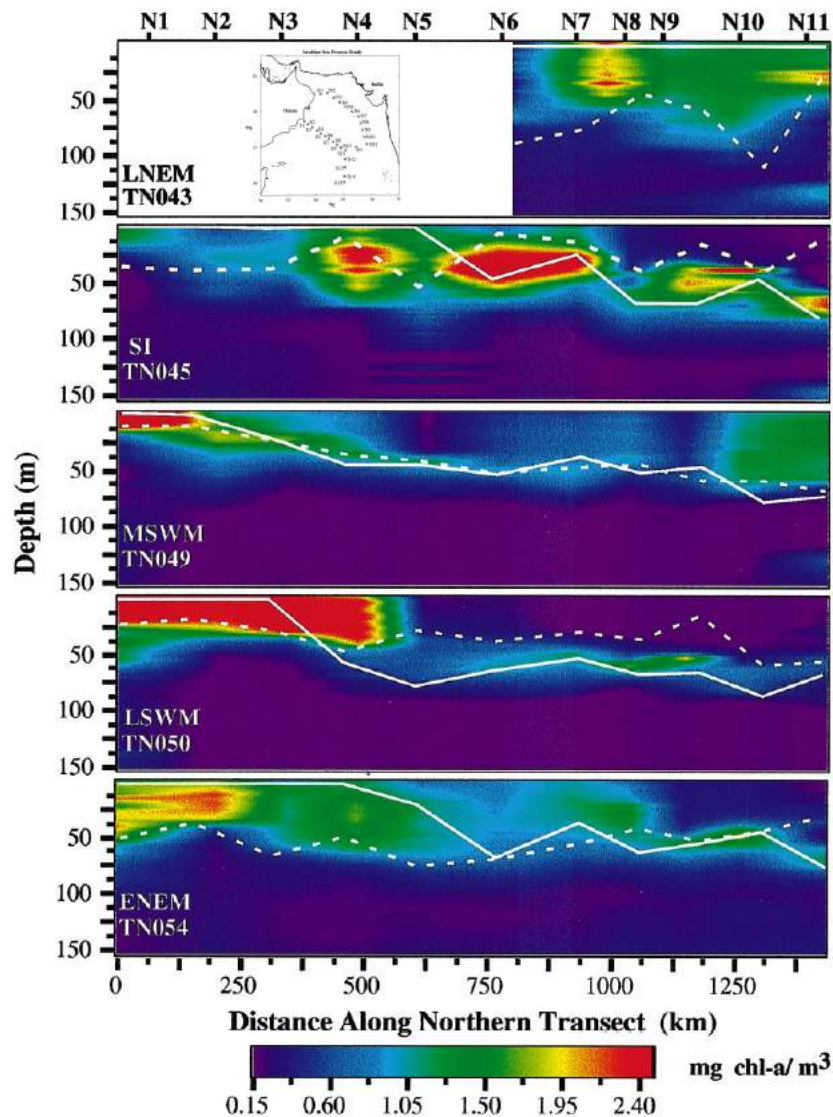


Figure 11: Chlorophyll sections of the northern transect (left panels) and southern transect (right panels) for each cruise. Mean MLD [$\Delta \sigma = 0.03$] (dotted line) and $0.5 \mu\text{M/l}$ nitrate isopleth (solid line) are shown for each cruise. The station locations are shown in the map inset in the upper left panel. Figures and caption modified from Gunderson et al. (1998).

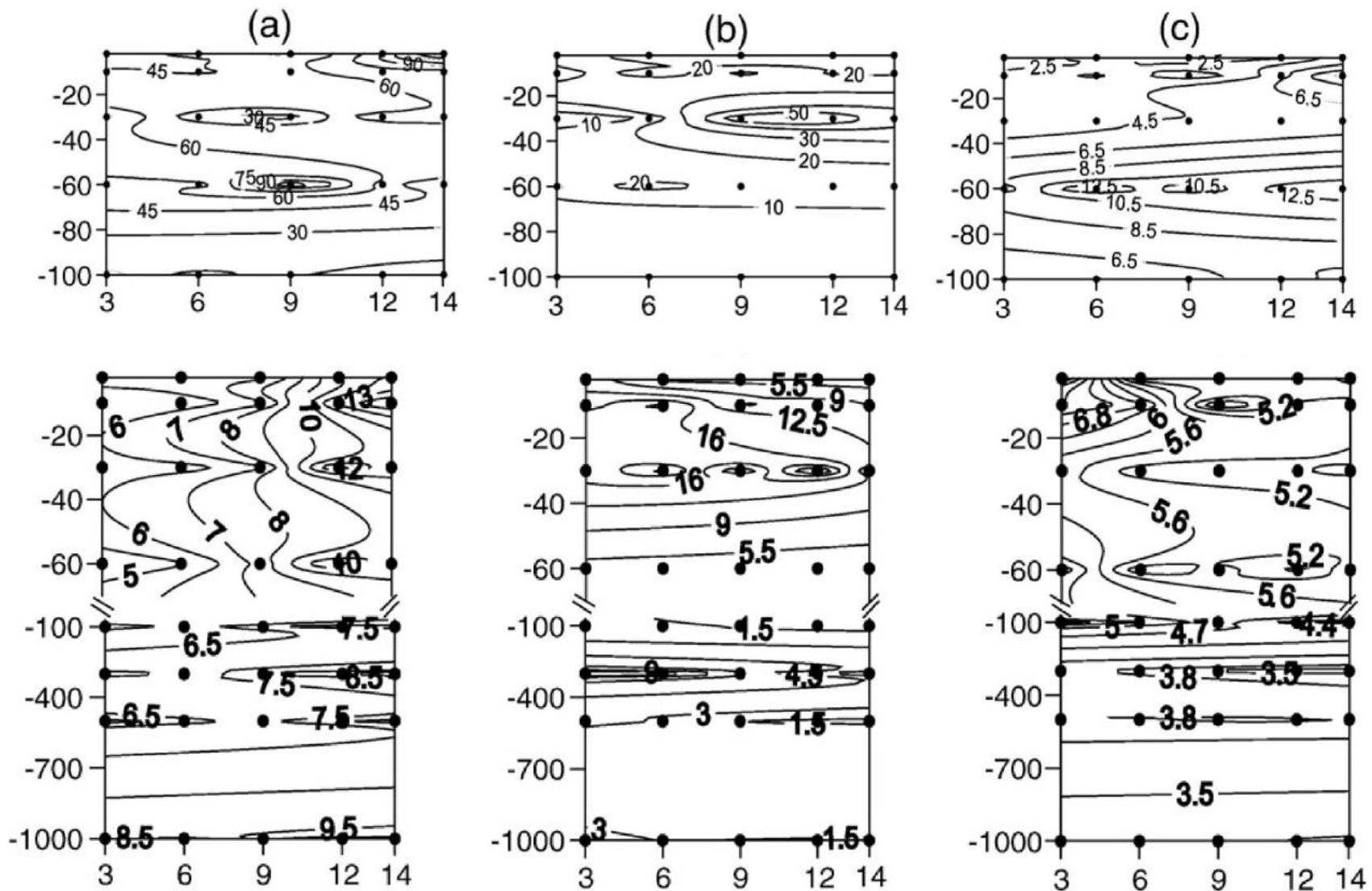


Figure 12: Distributions of chlorophyll a concentration (Chl a ng/l, top panels) and particulate organic carbon (POC $\mu\text{M C}$, bottom panels) in the central Bay of Bengal during (a) SWM, (b) FIM and (c) SPIM. Figure and caption modified from Fernandes et al. (2009).

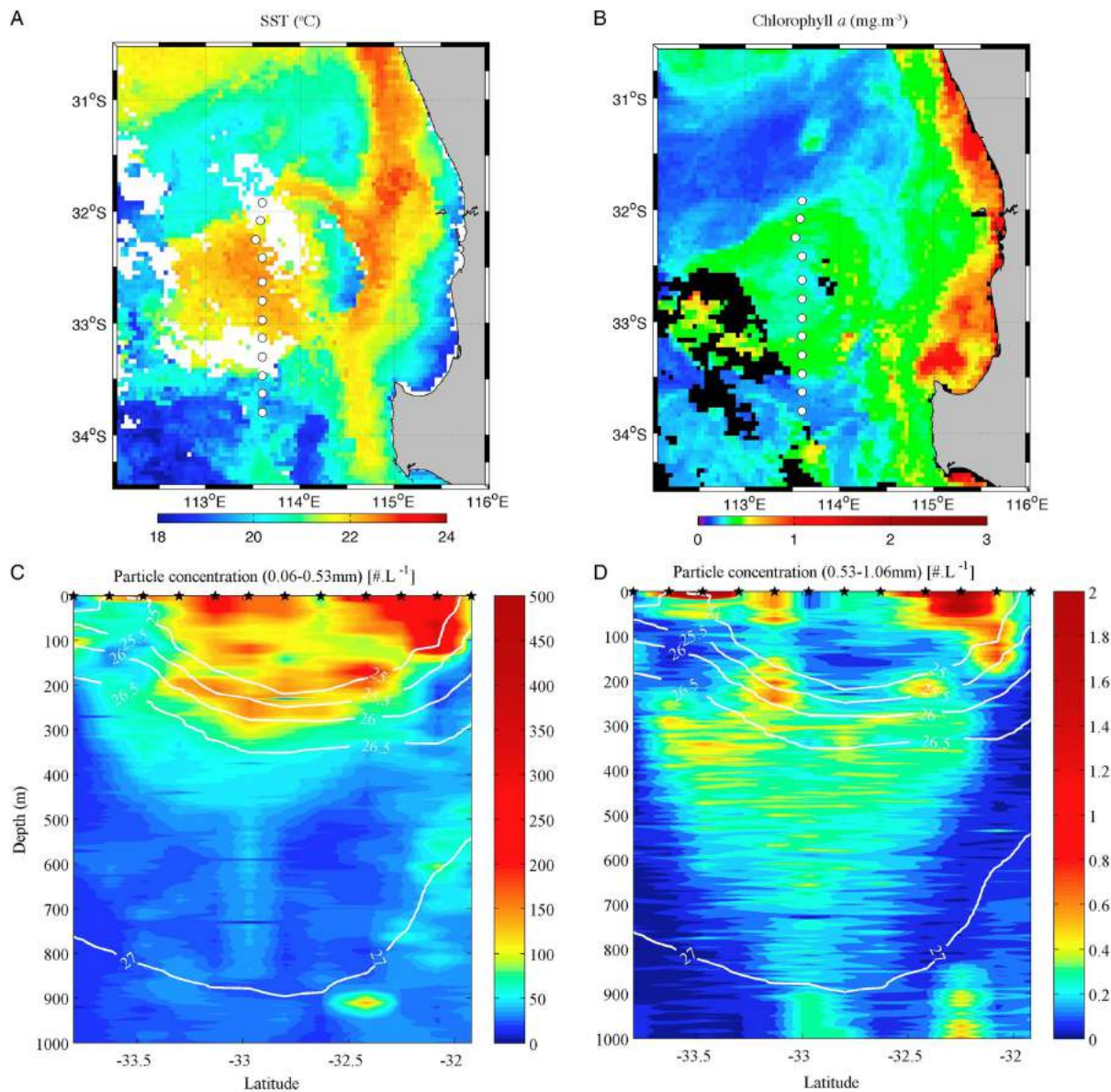


Figure 13: (a) Sea-surface temperature (°C) and (b) chlorophyll *a* (mg m⁻³) derived from Moderate Resolution Imaging Spectroradiometer (MODIS) satellite, showing the mesoscale eddy in the Leeuwin Current (LC) off Australia. White circles indicate stations sampled. Spatial distributions of particles across the eddy: (c) Small (0.06–0.5 mm) and (d) large (0.5–1 mm) particles shown in color, with isopycnals contoured in white. Figures and caption modified from Waite et al. (2016).